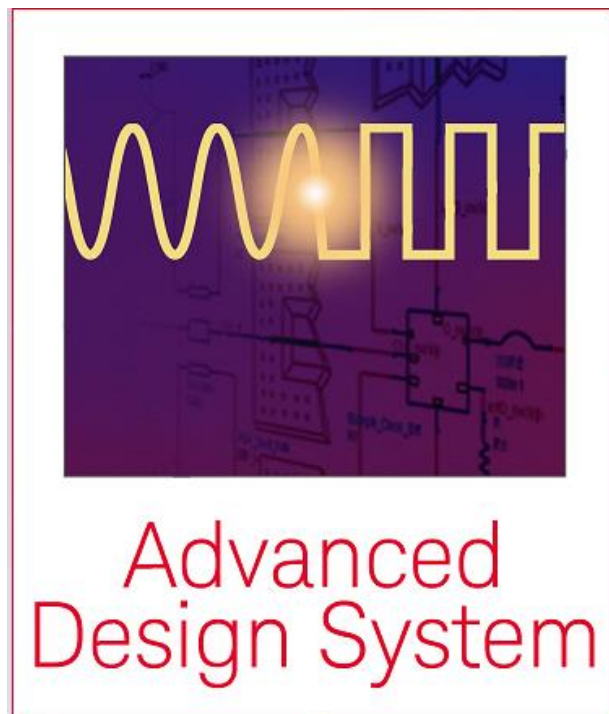


# RF and Microwave Circuit Design

A Design Approach Using (**ADS**)

## Chapter 4: Resonant Circuits and Filters



Ali Behagi

# RF and Microwave Circuit Design A Design Approach Using (ADS)

## **Chapter 4: Resonant Circuits and Filters**

Copyright ©2015 by Ali A. Behagi

Published in USA  
Techno Search  
Ladera Ranch, CA 92694

All rights reserved. Printed and bound in the United States of America. No part of this book may be reproduced, stored in a retrieval system, transmitted in any form or by any means, electronic, recording, or photocopying without prior permission in writing from the publisher.

---

## Chapter 4 Table of Contents

<b>Chapter 4: Resonant Circuits and Filters</b>	<b>4</b>
<b>4.1 Introduction</b>	
<b>4.2 Resonant Circuits</b>	<b>4</b>
4.2.1 Series Resonant Circuits	4
4.2.2 Parallel Resonant Circuits	7
4.2.3 Resonant Circuit Loss	9
4.2.4 Loaded Q and External Q	10
<b>4.3 Lumped Element Parallel Resonator Design</b>	<b>11</b>
4.3.1 Effect of Load Resistance on Bandwidth and $Q_L$	13
<b>4.4 Lumped Element Resonator Decoupling</b>	<b>14</b>
4.4.1 Design of the Tapped Capacitor Resonator	
4.4.2 Design of the Tapped Inductor Resonator	16
<b>4.5 Practical Microwave Resonators</b>	<b>18</b>
4.5.1 Transmission Line Resonators	19
4.5.2 Microstrip Resonator Example	22
4.5.3 ADS Model of the Microstrip Resonator	23
<b>4.6 Resonator Series Reactance Coupling</b>	<b>26</b>
4.6.1 One Port Microwave Resonator Analysis	28
<b>4.7 Filter Design at RF and Microwave Frequency</b>	<b>31</b>
4.7.1 Filter Topology	31
4.7.2 Filter Order	33
4.7.3 Filter Type	34
4.7.4 Filter Return Loss and Passband Ripple	36
<b>4.8 Lumped Element Filter Design</b>	<b>39</b>
4.8.1 Low Pass Filter Design Example	40
4.8.2 Physical Model of the Low Pass Filter in ADS	44
4.8.3 High Pass Filter Design Example	465
4.8.4 Physical Model of the High Pass Filter in ADS	49
<b>4.9 Distributed Filter Design</b>	<b>49</b>
4.9.1 Microstrip Stepped Impedance Low Pass Filter Design	49
4.9.2 Lumped Element to Distributed Element Conversion	51
4.9.3 EM Analysis of the Stepped Impedance Filter	56
4.9.4 Microstrip Coupled Line Filter Design	60
4.9.5 EM Analysis of the Edge Coupled Line Filter	71
<b>References, Problems, About the Author</b>	<b>65--68</b>

# Chapter 4

## Resonant Circuits and Filters

### 4.1 Introduction

The first half of this chapter examines resonant circuits. The second half is an introduction to the vast subject of filter networks. In the first half we discuss the lumped and distributed element resonant circuits and the equivalent networks of mechanical resonators. Resonant circuits are used in many applications such as filters, oscillators, tuners, tuned amplifiers, and microwave communication networks. The analysis of basic series and parallel RLC resonant circuits is implemented using the Keysight ADS software. The discussion turns to microwave resonators with an analysis of the Q factor and transmission line resonators. In the second half of the chapter the design of lumped element filters is followed by an introduction to distributed element filters. The chapter concludes with the design of microstrip stepped impedance and microstrip coupled line filters. In the analysis and design of all resonant and filter networks the use of Keysight ADS software is demonstrated.

### 4.2 Resonant Circuits

Near resonance, RF and microwave resonant circuits can be represented either as a lumped element series or parallel RLC networks.

#### 4.2.1 Series Resonant Circuits

In this section we analyze the behavior of the series resonant circuits in ADS.

**Example 4.2-1:** Consider the one port series resonator that is represented as a series RLC circuit of Figure 4-1. Analyze the circuit, with  $R = 10 \Omega$ ,  $L = 10 \text{ nH}$ , and  $C = 10 \text{ pF}$ .

**Solution:** The procedure for ADS analysis is as follows. This procedure will be repeated throughout the book.

- Start ADS and create a new workspace
- Name the workspace Ex4.2-1\_wrk
- From the Main window create a new schematic in cell\_1
- In the schematic window, click Insert > Template > ads-templates:S\_Params
- Delete the DisplayTemplate icon
- Place R, L, and C elements from the Lumped-Components palette on the schematic and connect them as shown in Figure 4-1.
- Set R=10  $\Omega$ , L=10 nH, and C=10 pF
- Type in Zin in the part selection box and place it on the schematic to measure the input impedance of the circuit.
- Set the frequency range from 450 to 550 MHz in 1 kHz step and wire up the schematic as shown in Figure 4-1

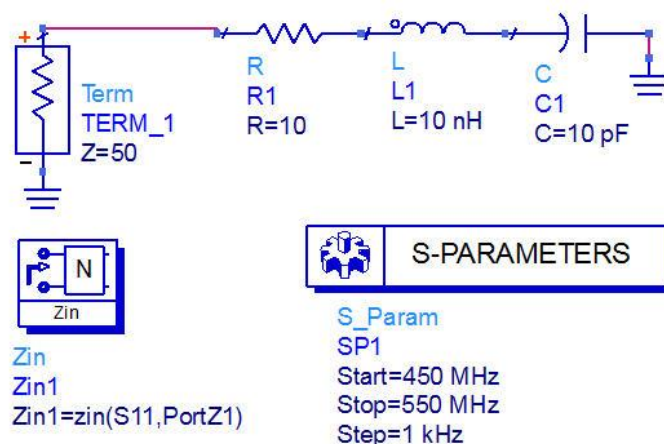


**Figure 4-1** One-port series RLC resonator circuit

The plot of the resonator's input impedance in Figure 4-2 shows that the resonance frequency is about 503.3 MHz and the input impedance at resonance is 10  $\Omega$ , the value of the resistor in the network.

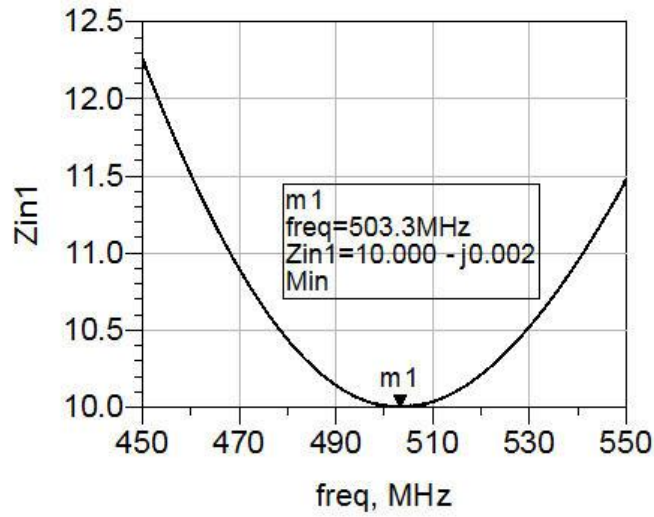


**Figure 4-2** Input impedance showing the resonance frequency at m1

The input impedance of the series RLC resonant circuit is given by,

$$Z_{in} = R + j\omega L - j\frac{1}{\omega C}$$

where,  $\omega = 2\pi f$  is the angular frequency in radian per second.

If the AC current flowing in the series resonant circuit is  $I$ , then the complex power delivered to the resonator is

$$P_{in} = \frac{|I|^2}{2} Z_{in} = \frac{|I|^2}{2} \left( R + j\omega L - j\frac{1}{\omega C} \right) \quad (4-1)$$

At resonance the reactive power of the inductor is equal to the reactive power of the capacitor. Therefore, the power delivered to the resonator is equal to the power dissipated in the resistor

$$P_{in} = \frac{|I|^2 R}{2} \quad (4-2)$$

## 4.2.2 Parallel Resonant Circuits

**Example 4.2-2:** Analyze a rearrangement of the RLC components of Figure 4-1 into the parallel configuration of Figure 4-3. The schematic of Figure 4-3 represents the lumped element representation of the parallel resonant circuit.

**Solution:** The one port parallel resonant circuit is shown in Figure 4-3.

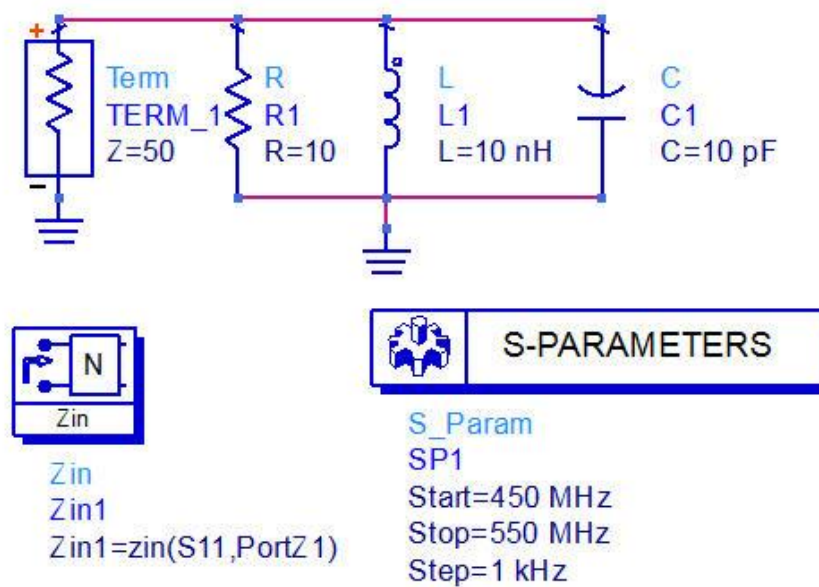


**Figure 4-3** One-port parallel RLC resonant circuit

Simulate the schematic and display the input impedance in a rectangular plot. The plot of the magnitude of the input impedance shows that the resonance frequency is still 503.3 MHz where the input impedance is  $R = 10 \Omega$ . Again this shows that the impedance of the inductor cancels the impedance of the capacitor at resonance. In other words, the reactance,  $X_L$ , is equal to the reactance,  $X_C$ , at the resonance frequency.

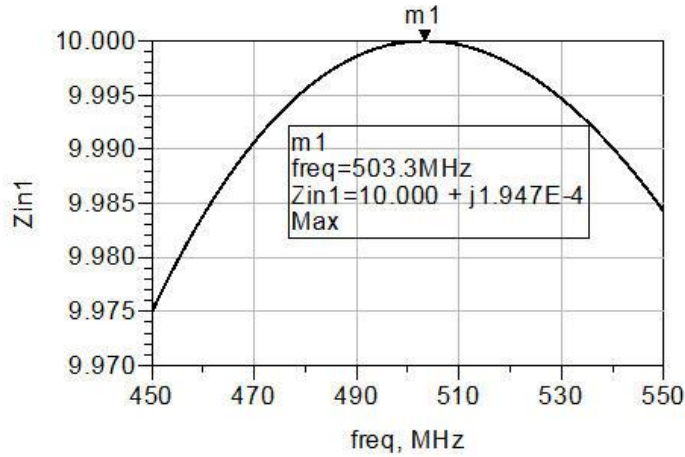


**Figure 4-4** Input impedance of parallel RLC resonant circuit

The input admittance of the parallel resonant circuit is given by:

$$Y_{IN} = \frac{1}{R} + j\omega C - j\frac{1}{\omega L}$$

If the AC voltage across the parallel resonant circuit is  $V$ , then the complex power delivered to the resonator is

$$P_{in} = \frac{|V|^2}{2} Y_{in} = \frac{|V|^2}{2} \left( \frac{1}{R} + j\omega C - j\frac{1}{\omega L} \right) \quad (4-3)$$

At resonance the reactive power of the inductor is equal to the reactive power of the capacitor. Therefore, the power delivered to the resonator is equal to the power dissipated in the resistor

$$P_{in} = \frac{|V|^2}{2R} \quad (4-4)$$

The resonance frequency for the parallel resonant circuit as well as the series resonant circuit is obtained from:



$$\omega_o = 2\pi f_o = \frac{1}{\sqrt{LC}} \quad (4-5)$$

where,  $\omega_o$  is the angular frequency in radian per second and  $f_o$  is equal to the frequency in Hertz.

### 4.2.3 Resonant Circuit Loss

In Figures 4-1 and 4-3 the resistor R1 represents the loss in the resonator. It includes the losses in the capacitor as well as the inductor. The Q factor can be shown to be a ratio of the energy stored in the inductor and capacitor to the power dissipated in the resistor as a function of frequency <sup>[6]</sup>. For the series resonant circuit of Figure 4-1 the unloaded Q factor is defined by:

$$Q_u = \frac{X}{R} = \frac{\omega_o L}{R} = \frac{1}{\omega_o RC} \quad (4-6)$$

The unloaded Q factor of the parallel resonant circuit in Figure 4-3 is simply the inverse of the unloaded Q factor of the series resonant circuit.

$$Q_u = \frac{R}{X} = \frac{R}{\omega_o L} = \omega_o RC \quad (4-7)$$

We can clearly see that as the resistance increases in the series resonant circuit, the Q factor decreases. Conversely as the resistance increases in the parallel resonant circuit, the Q factor increases.

The Q factor is a measure of loss in the resonant circuit. Thus a higher Q corresponds to lower loss and a lower Q corresponds to a higher loss. It is usually desirable to achieve high Q factors in a resonator as it will lead to lower losses in filter applications or lower phase noise in oscillators. Note that the resonator Q of Equation (4-6) and (4-7) is defined as  $Q_u$ , the unloaded Q of the resonator. This means that the resonator is not connected to any load.

Equations (4-6) and (4-7) would then have to be modified to include the source and load resistance. We might also surmise that any reactance associated with the source or load impedance may alter the resonant frequency of the resonator. This leads to two additional definitions of Q factor that the engineer must consider: the loaded Q and the external Q.

#### 4.2.4 Loaded Q and External Q

Analyze the parallel resonator that is attached to a 50  $\Omega$  source and load as shown in Figure 4-5.

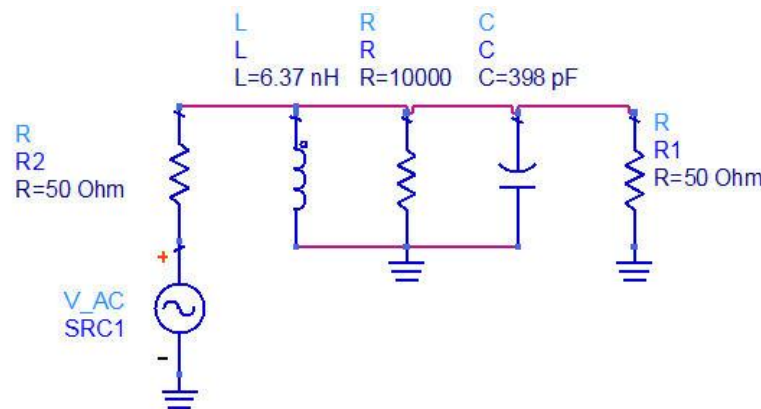


**Figure 4-5** Parallel resonator with source and load impedance

Using Equation (4-7) to define the Q factor for the circuit requires that we include the source and load resistance which is ‘loading’ the resonator. This leads to the definition of the loaded Q, or  $Q_L$ , for the parallel resonator as defined by Equation (4-8).

$$Q_L = \frac{R_S + R + R_L}{\omega_o L} \quad (4-8)$$

Conversely we can define a Q factor in terms of only the external source and load resistance. This leads to the definition of the external Q, or  $Q_E$ .

$$Q_E = \frac{R_S + R_L}{\omega_o L} \quad (4-9)$$

The three Q factors are related by the inverse relationship of Equation (4-10).

$$\frac{1}{Q_L} = \frac{1}{Q_E} + \frac{1}{Q_U} \quad (4-10)$$

At RF and microwave frequencies it is difficult to directly measure the  $Q_u$  of a resonator. We may be able to calculate the Q factor based on the physical properties of the individual inductors and capacitors as we have seen in chapter 1. This is usually quite difficult and the Q factor is typically measured using a Vector Network Analyzer, VNA. Therefore, the measured Q factor is usually the loaded Q, or  $Q_L$ . External Q is often used with oscillator circuits that are generating a signal. In this case the oscillator's load impedance is varied so that the external Q can be measured. The loaded Q of the network is then related to the fractional bandwidth by Equation (4-11) <sup>[8]</sup>.

$$Q_L = \frac{\sqrt{f_l f_h}}{BW_{-3dB}} \quad (4-11)$$

where, BW is the -3 dB bandwidth,  $f_l$  and  $f_h$  are the lower and upper frequencies in Hz at -3dB points.

### 4.3 Lumped Element Parallel Resonator Design

**Example 4.3-1:** In this example we design a lumped element parallel resonator at a frequency of 100 MHz. The resonator is intended to operate between a source resistance of 100  $\Omega$  and a load resistance of 400  $\Omega$ .

**Solution:** Best accuracy would be obtained by using S-parameter files or Modelithics models for the inductor and capacitor. However a good first order model can be obtained by using the ADS inductor and capacitor models that include the component Q factor. These models save us the work of calculating

the equivalent resistive part of the inductor and capacitor model. The component Q factors are shown in the schematic of Figure 4-6.

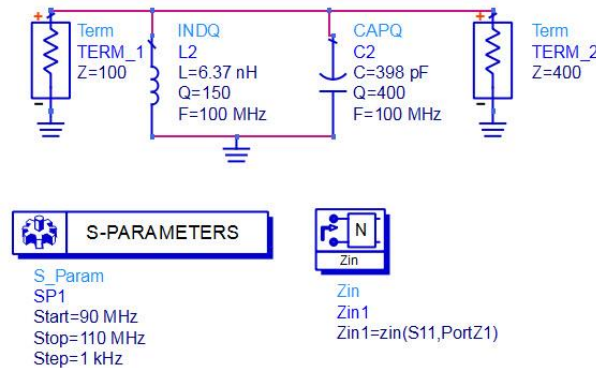


**Figure 4-6** Parallel resonator using components with assigned Q factors

Simulate the schematic and display the insertion loss in a rectangular plot.

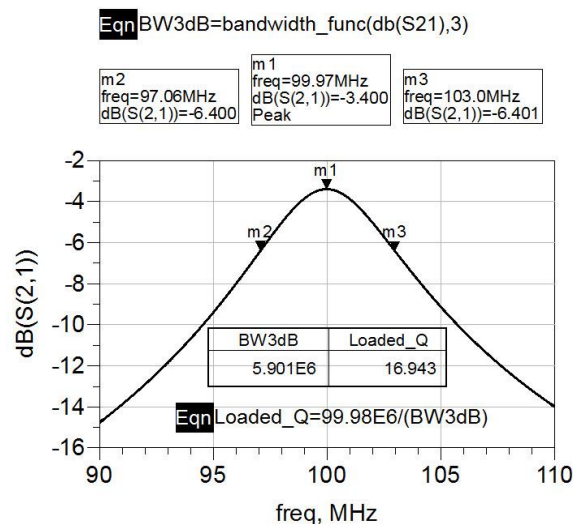


**Figure 4-7** Insertion loss and calculation of 3 dB bandwidth and Q factor

Note that markers have been placed on the plot of the insertion loss, S21, that gives readout of -3 dB bandwidth. To place markers m2 and m3 manually at -3dB points, first place marker m1 at the peak of S21 trace. Next place marker m2 at a point below marker m1. Select marker m2 and press the up and down arrows to move the marker m2 as close to -3dB point as possible. Repeat the

process for marker m3. The loaded Q can be calculated using Equation (4-11).

$$Q_L = \frac{\sqrt{f_l f_h}}{BW} = \frac{99.98 \text{ MHz}}{5.901 \text{ MHz}} = 16.94$$

The designer must use caution when sweeping resonant circuits. Particularly high Q band pass networks require a large number of discrete frequency steps in order to achieve the necessary resolution required to accurately measure the 3dB bandwidth. The ADS measurement function `bandwidth_func(db(S21),3)` also measures the 3 dB bandwidth very accurately.

### 4.3.1 Effect of Load Resistance on Bandwidth and $Q_L$

In RF circuits and systems the impedances encountered are often quite low, ranging from 1  $\Omega$  to 50  $\Omega$ . It may not be practical to have a source impedance of 100  $\Omega$  and a load impedance of 400  $\Omega$ . In the next section we replace these impedances with 50 Ohm resistors.

**Example 4.3-2:** In the parallel LC Example 4.3-1, change the load from 400  $\Omega$  to 50  $\Omega$  and re-examine the circuit's 3 dB bandwidth and  $Q_L$ .

**Solution:** Change the load resistance from 400  $\Omega$  to 50  $\Omega$  as shown in Figure 4-8.

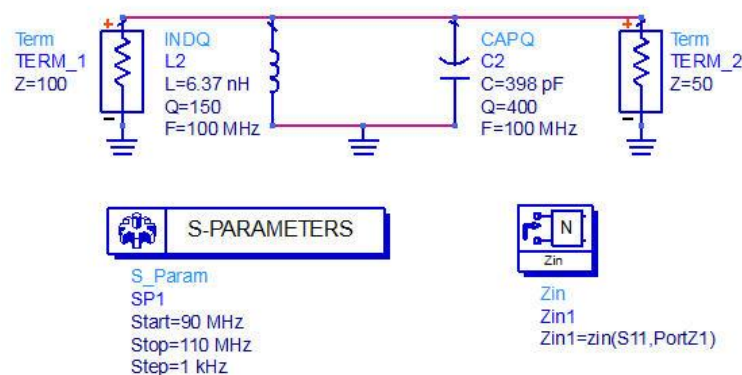


**Figure 4-8** Parallel resonance circuit

Simulate the schematic and display the insertion loss in a rectangular plot. In ADS the bandwidth\_func() function uses an iterative process to interpolate between simulated points.

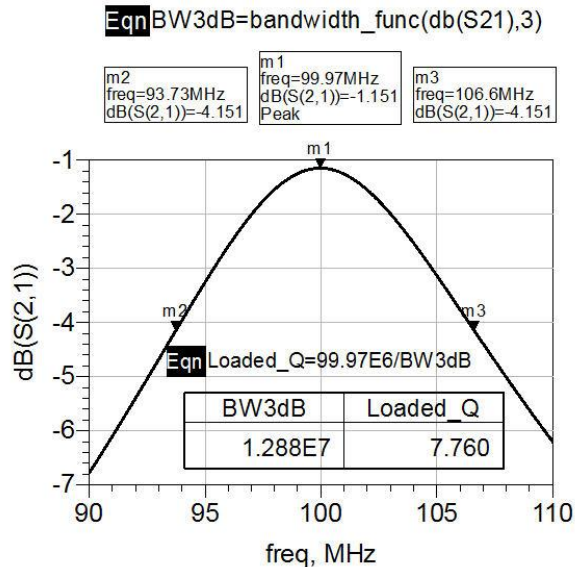


**Figure 4-9** Insertion loss of parallel resonance circuit

Notice the 3 dB bandwidth is now 12.88 MHz resulting in a loaded Q factor of 7.76.

$$Q_L = \frac{\sqrt{f_l f_h}}{BW} = \frac{99.958 \text{ MHz}}{12.88 \text{ MHz}} = 7.76$$

The loaded Q factor has decreased by nearly half of the original value. We have increased the bandwidth or de-Q'd the resonator. This can also be thought of as tighter coupling of the resonator to the load.

#### 4.4 Lumped Element Resonator Decoupling

To maintain the high Q of the resonator when attached to a load such as 50  $\Omega$ , it is necessary to transform the low impedance to high impedance presented to the load. The 50  $\Omega$  impedance can be transformed to the higher impedance of the parallel resonator thereby resulting in less loading of the resonator impedance. This is referred to as loosely coupling the resonator to the load. The tapped-capacitor and tapped-inductor networks can be used to accomplish

this Q transformation in lumped element circuits.

#### 4.4.1 Design of the Tapped Capacitor Resonator

**Example 4.4-1:** Consider rearranging the parallel LC network of Figure 4-8 with the tapped capacitor network shown in Figure 4-10. Re-examine the circuit's 3 dB bandwidth and  $Q_L$ .

**Solution:** The new capacitor values for C1 and C2 can be found by the simultaneous solution of the following equations <sup>[2]</sup>.

$$C_T = \frac{C_1 \cdot C_2}{C_1 + C_2} \quad (4-12)$$

$$R_{L1} = R_L \left( 1 + \frac{C_1}{C_2} \right)^2 \quad (4-13)$$

$R_{L1}$  is the higher, transformed, load resistance. In this example substitute  $R_{L1} = 400 \Omega$ , the original load resistance value.  $C_T$  is simply the original capacitance of 398 pF. The capacitor values are found to be:  $C_1 = 1126.23 \text{ pF}$  and  $C_2 = 616.1 \text{ pF}$ . The new resonator circuit is shown in Figure 4-10.

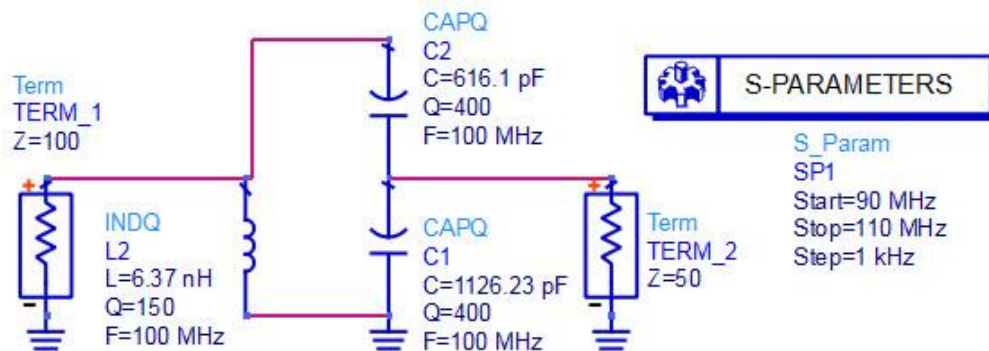


**Figure 4-10** Parallel LC resonator using tapped capacitor

Sweeping the circuit we see that the response has returned to the original performance of Figure 4-7.

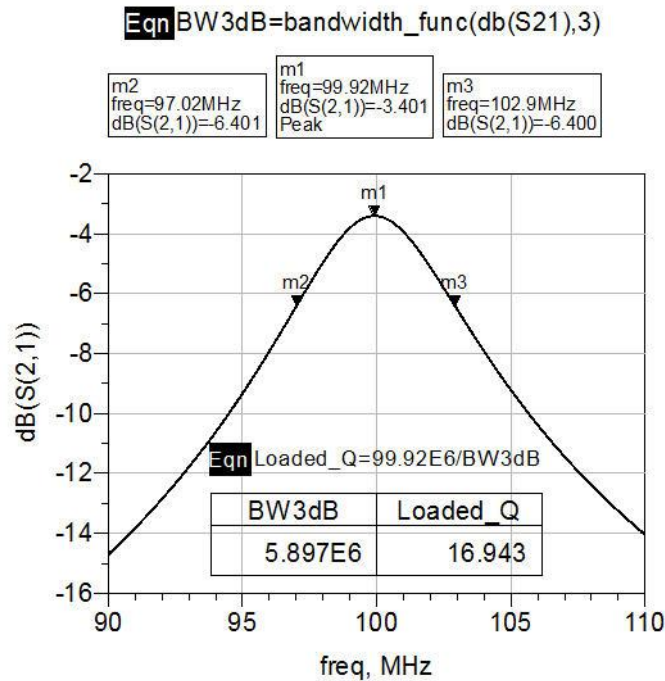


**Figure 4-11** Response of parallel LC resonator using a tapped capacitor

The 3 dB bandwidth has returned to 5.89 MHz making the  $Q_L$  equal to:

$$Q_L = \frac{\sqrt{f_i f_h}}{BW} = \frac{99.92 \text{ MHz}}{5.897 \text{ MHz}} = 16.94$$

The  $50 \Omega$  load resistor has been successfully decoupled from the resonator. The tapped capacitor and inductor resonators are popular methods of decoupling RF and lower microwave frequency resonators. It is frequently seen in RF oscillator topologies such as the Colpitts oscillator in the VHF frequency range.

#### 4.4.2 Design of the Tapped Inductor Resonator

**Example 4.4-2:** Similarly design a tapped inductor network to decouple the  $50 \Omega$  source impedance from loading the resonator.

**Solution:** Replace the  $100 \Omega$  source impedance with a  $50 \Omega$  source and use a



tapped inductor network to transform the new  $50\ \Omega$  source to  $100\ \Omega$ . Modify the circuit to split the  $6.37\ \text{nH}$  inductor,  $L_T$ , into two series inductors,  $L_1$  and

$L_2$ . The inductor values can then be calculated by solving the following equation set simultaneously [2].  $R_{S1}$  is the higher, transformed, source resistance. In this example substitute  $R_{S1} = 100\ \Omega$ ,

$$R_{S1} = R_S \left( \frac{L_T}{L_1} \right)^2 \quad (4-14)$$

$$L_T = L_1 + L_2 \quad (4-15)$$

Solving the equation set results in values of  $L_1=4.5\ \text{nH}$  and  $L_2=1.87\ \text{nH}$ . The resulting schematic and response are shown in Figures 4-12 and 4-13.

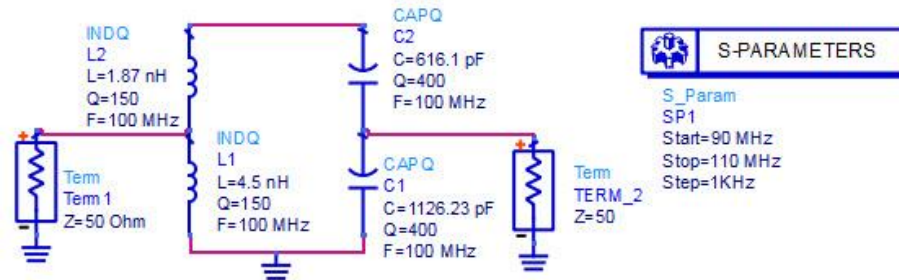


**Figure 4-12** Tapped-inductor parallel resonant circuit

The new response is identical to the plot of Figure 4-7. Therefore we now have a source and load resistance of  $50\ \Omega$  and have not reduced the  $Q$  of the resonator from what we had with the original source resistance of  $100\ \Omega$  and a load resistance of  $400\ \Omega$ .

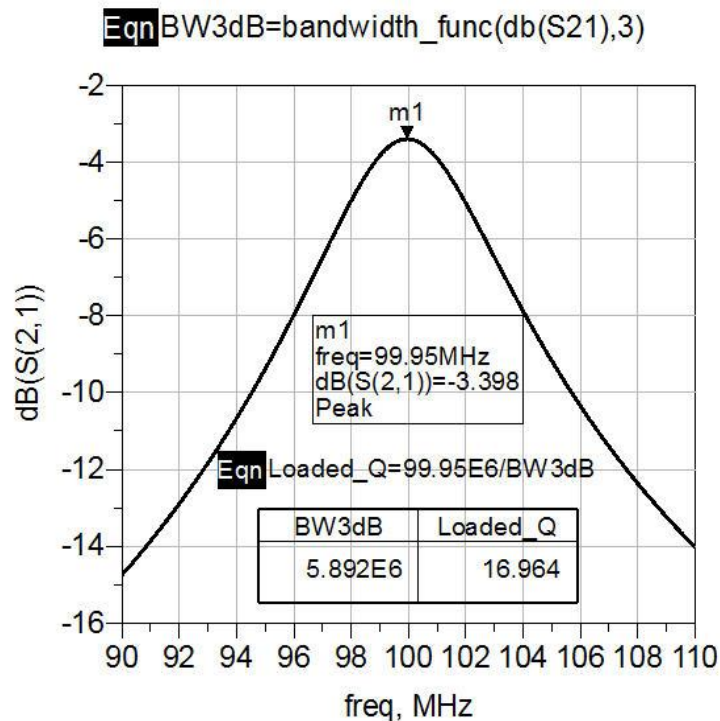


**Figure 4-13** Response of the parallel resonant circuit

## 4.5 Practical Microwave Resonators

At higher RF and microwave frequencies resonators are seldom realized with discrete lumped element RLC components. This is primarily due to the fact that the small values of inductance and capacitance are physically unrealizable. Even if the values could be physically realized we would see that the resulting Q factors would be unacceptably low for most applications. Microwave resonators are realized in a wide variety of physical forms. Resonators can be realized in all of the basic transmission line forms that were covered in Chapter 2. There are many specialized resonators such as ceramic dielectric resonator pucks that are coupled to a microstrip transmission line as well as Yittrium Iron Garnet spheres that are loop coupled to its load. These resonators are optimized for very high Q factors and may be tunable over a range of frequencies.

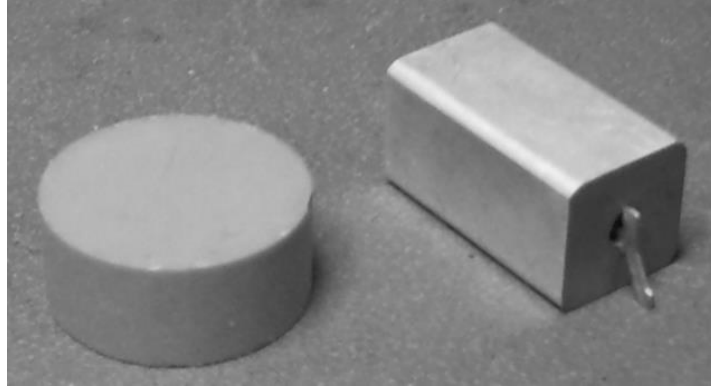


**Figure 4-14** Ceramic dielectric resonator (puck) and coaxial resonator

### 4.5.1 Transmission Line Resonators

From Figure 2-20 we have seen that a quarter-wave short-circuited transmission line results in a parallel resonant circuit. Similarly Figure 2-22 showed that a half-wave open circuited transmission line results in a parallel resonant circuit. Such parallel resonant circuits are often used as one port resonators. Near the resonant frequency, the one port resonator behaves as a parallel RLC network as shown in Figure 4-2. As the frequency moves further from resonance the equivalent network becomes more complex typically involving multiple parallel RLC networks. One port resonators are coupled to one another to form filter networks or directly to a transistor to form a microwave oscillator. Knowing the losses due to the physical and electrical parameters of the transmission line, one can calculate the  $Q_u$  of the transmission line resonator. The microstrip resonator  $Q_u$  is comprised of losses due to the conductor metal, the substrate dielectric, and radiation losses. The  $Q_u$  is often dominated by the conductor  $Q$ . Unfortunately it can be quite difficult to accurately determine the conductor losses in a microstrip resonator. T. C. Edwards has developed a set of simplified expressions for the conductor losses <sup>[4]</sup>. Equation (4-16) is an approximation of the conductor losses that treats the transmission line as a perfectly smooth surface.

$$\alpha_c = 0.072 \frac{\sqrt{f}}{W_e Z_o} \lambda_g \quad \text{dB/inch} \quad (4-16)$$

Where:

$f$  = the frequency in GHz  
 $W_e$  = the effective conductor width (inches)  
 $Z_o$  = the characteristic impedance of the line  
 $\alpha_c$  = Conductor loss in dB/inch  
 $\lambda_g$  = wavelength in dielectric in inches

A microstrip conductor is actually not perfectly smooth but exhibits a certain roughness. The surface roughness exists on the bottom of the microstrip conductor where it contacts the dielectric. This can be seen by magnifying the cross section of a microstrip line's contact with the dielectric material. The surface roughness is usually specified as an r.m.s. value.

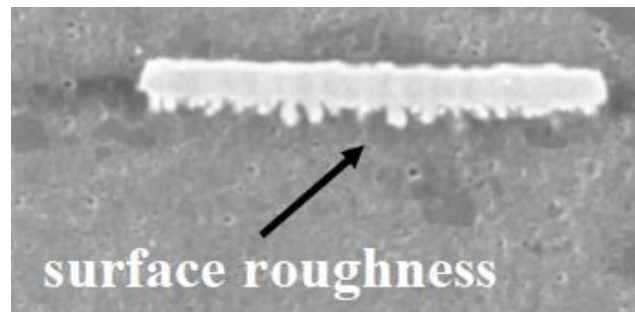


**Figure 4-15** Cross section of microstrip line showing surface roughness at the conductor to dielectric interface (courtesy of Tektronix)

Edwards modified Equation (4-16) to include the effects of the surface roughness as given by Equation (4-17).

$$\alpha'_c = \alpha_c \left[ 1 + \frac{2}{\pi} \tan^{-1} \left( 1.4 \left( \frac{\Delta}{\delta_s} \right)^2 \right) \right] \quad \text{dB/inch} \quad (4-17)$$

where,  $\Delta$  is the r.m.s. surface roughness and  $\delta_s$  is the conductor skin depth. The corresponding Q factor related to the conductor is then given by:

$$Q_c = \frac{27.3 \sqrt{\epsilon_{eff}}}{\alpha_c \lambda_o} \quad (4-18)$$

The dielectric loss is determined by the dielectric constant and loss tangent. It is calculated using Equation (4-19).

$$\alpha_d = 27.3 \frac{\epsilon_r (\epsilon_{eff} - 1) \tan \delta}{\sqrt{\epsilon_{reff}} (\epsilon_r - 1) \lambda_o} \quad \text{dB/inch} \quad (4-19)$$

where:

$\epsilon_r$  = the substrate dielectric constant

$\epsilon_{reff}$  = the effective dielectric constant

$\tan \delta$  = the loss tangent of the dielectric

$\lambda_o$  = wavelength in inches

The corresponding Q factor due to the dielectric is then given by:

$$Q_d = 27.3 \frac{\sqrt{\epsilon_{eff}}}{\alpha_d \lambda_o} \quad (4-20)$$

We know that a microstrip line will also have some radiation of energy from the top side of the line. The open circuit stub will also experience some radiation effect from the open circuited end. On low dielectric constant substrates,  $\epsilon_r \leq 4.0$ , the radiation losses are more significant for high impedance lines. Conversely for high dielectric constant substrates,  $\epsilon_r \geq 10$ , low impedance lines experience more radiation loss<sup>[10]</sup>. The radiation Q factor is presented as Equation (4-21)<sup>[9]</sup>.

$$Q_r = \frac{Z_o(f)}{480\pi \left(\frac{h}{\lambda_o}\right)^2 \left\{ \left[ \frac{\epsilon_{eff}(f) + 1}{\epsilon_{eff}(f)} \right] - \left[ \frac{(\epsilon_{eff}(f) - 1)^2}{2(\epsilon_{eff}(f))^{3/2}} \ln \left( \frac{\sqrt{\epsilon_{eff}(f)} + 1}{\sqrt{\epsilon_{eff}(f)} - 1} \right) \right] \right\}} \quad (4-21)$$

where, h = substrate thickness in cm.

Note that in Equation (4-21) the line impedance and effective dielectric constant are defined as functions of frequency. This includes the dispersion or frequency dependent effect of  $Z_o$  and  $\epsilon_{eff}$ . Dispersion tends to slightly increase the  $\epsilon_{eff}$  as the frequency increases. This dispersive  $Z_o$  and  $\epsilon_{eff}$  are given in Equations (4-22) and (4-23).

$$\epsilon_{eff(f)} = \frac{\epsilon_r - \epsilon_{eff}}{1 + \left[ (0.6 + 0.009Z_o) \left( \frac{f}{Z_o / 8\pi(h - 2t)} \right)^2 \right]} \quad (4-22)$$

where,

h = substrate thickness in mils

t = conductor thickness in mils

$$Z_{o(f)} = Z_o \sqrt{\frac{\epsilon_{eff}}{\epsilon_{eff(f)}}} \quad (4-23)$$

Finally the resultant overall unloaded Q factor,  $Q_u$ , of the microstrip line can be determined by the reciprocal relationship of Equation (4.24).

$$\frac{1}{Q_u} = \frac{1}{Q_c} + \frac{1}{Q_d} + \frac{1}{Q_r} \quad (4-24)$$

## 4.5.2 Microstrip Resonator Example

**Example 4.5-1:** Design a 5 GHz half wavelength open circuit microstrip resonator. The resonator is realized with a 50  $\Omega$  microstrip line on Roger's RO3003 dielectric. Calculate the unloaded Q factor of the resonator. The substrate parameters are defined as:

Dielectric constant	$\epsilon_r = 3$
Substrate height	h = 0.030 in.
Conductor thickness	t = .0026 in.
Line Impedance	$Z_o = 50 \Omega$
Conductor width	w = 0.077 in.
Loss tangent	$\tan\delta = 0.0013$

**Solution:** Using the simplified expression of Equation (4-16) for a smooth microstrip line the conductor loss and Q factor is calculated as:

$$\alpha_c = 0.072 \frac{\sqrt{5}}{0.077(50)} (1.52) = 0.063 \text{ dB/inch}$$

$$Q_c = \frac{27.3\sqrt{2.41}}{(0.063)(2.36)} = 283.1$$

The dielectric loss and Q factor are then calculated from Equation (4-19) and (4-20).

$$\alpha_d = 27.3 \frac{(3)(2.41-1)(0.0013)}{\sqrt{2.41}(3-1)(2.36)} = 0.021 \text{ dB/inch}$$

$$Q_d = 27.3 \frac{\sqrt{2.41}}{(0.021)(2.36)} = 875.2$$

For simplicity the radiation Q factor will be omitted. We will model the resonator using the ADS Linear simulator. Linear simulators often do not model the radiation effects of the microstrip line. Therefore the overall unloaded Q factors then becomes.

$$\frac{1}{Q_u} = \frac{1}{283.1} + \frac{1}{875.2} = \frac{1}{213.9}$$

$$Q_u = 213.9$$

### 4.5.3 ADS Model of the Microstrip Resonator

The half wave open-circuited microstrip resonator is modeled in ADS as shown in Fig 4-16. Note that the source and load impedance has been increased to  $5000 \Omega$  to avoid loading the impedance of the parallel resonant circuit. Perform a linear sweep of the resonator using 0.1 MHz step from 4500 MHz to 5400 MHz.

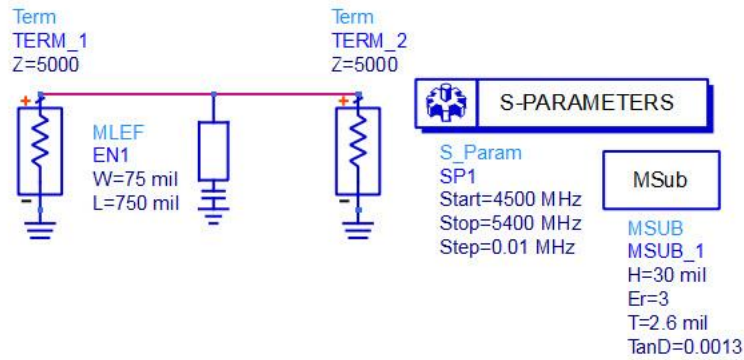


**Figure 4-16** Half-wave open ended microstrip resonator

Simulate the schematic and display the S21, the -3 dB bandwidth, and the loaded Q factor, as shown in Figure 4-17.

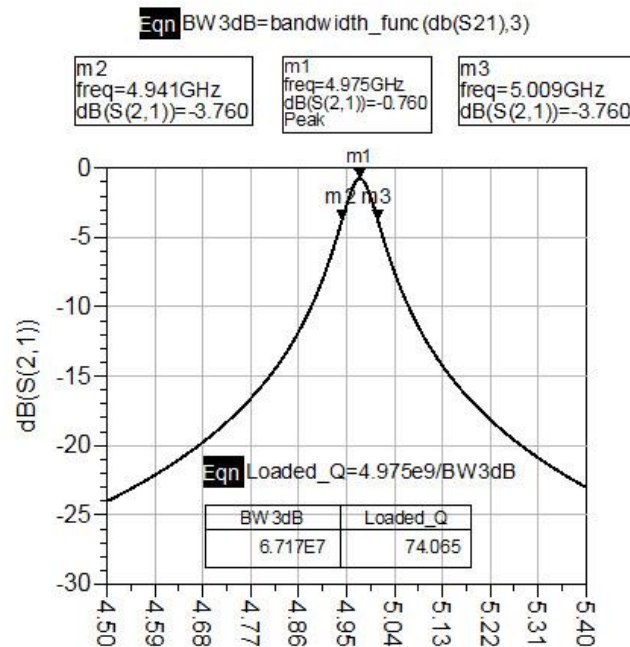


**Figure 4-17** Response of the half-wave open circuit microstrip resonator

Using the techniques of section 4.2.3 and Equation (4-10), the 3dB bandwidth is measured to determine the loaded Q of the resonator.

$$Q_L = \frac{4974.88\text{MHz}}{68\text{MHz}} = 73.16$$



The insertion loss at the resonant frequency can be used to relate the loaded Q factor to the  $Q_u$  as shown by Equation (4-25).

$$\text{InsertionLoss}(dB) = 20 \log \frac{Q_u}{Q_u - Q_L} \quad (4-25)$$

Or: 
$$0.76 = 20 \log \frac{Q_u}{Q_u - 73.16}$$

$$Q_u = 882.7$$

## 4.6 Resonator Series Reactance Coupling

To reduce the loading on the half wave resonator of Figure 4-16, the source and load impedances of  $5000 \Omega$  were used. In practice the resonator is typically coupled to lower impedance circuits. If we attempt to examine the resonator on a network analyzer, most modern test equipment will have  $50 \Omega$  impedance levels. Such resonators are often coupled to the circuit by a highly reactive circuit element. This reactive element can be realized as a series capacitor or inductor. The resonator is then analyzed as a one port network. As the frequency is swept over a narrow frequency range around the resonant frequency, a circle is formed on the Smith chart. This trace is known as the Q circle of the resonator <sup>[5]</sup>. Figure 4-19 shows the Smith chart plot of the resonator's input reflection coefficient, S11. Three plots are shown each with a different value of coupling capacitance. We can see that as the coupling capacitance changes, the resonant frequency of the circuit also changes. The series capacitance acts to decrease the overall resonance frequency of the circuit. This new resonance frequency is known as the loaded resonance frequency. Because the series capacitance lowers the frequency, the length of the resonator was decreased to 0.736 inches to return the resonant frequency close to 5 GHz. With the coupling capacitance set at 0.027 pF the Q circle passes through the center of the Smith chart at the resonant frequency. This is known as critical coupling and is characterized by having the lowest return loss on the scalar plot of Figure 4-20. With the capacitance increased to 0.05 pF the resonator is more strongly coupled to the  $50 \Omega$  load. The scalar plot shows that the resonance frequency is decreased. The Smith chart shows a

larger Q circle which is a characteristic of an over coupled resonator. With the coupling capacitor set to 0.015 pF the resonance frequency increases. The Smith chart shows that the Q circles become much smaller thus under coupling the resonator.

As Figure 4-20 shows, the value of the coupling capacitor also has an impact on the size of the Q circle. The diameter of the Q circle is dependent on the coupling of the resonator to the 50  $\Omega$  source.

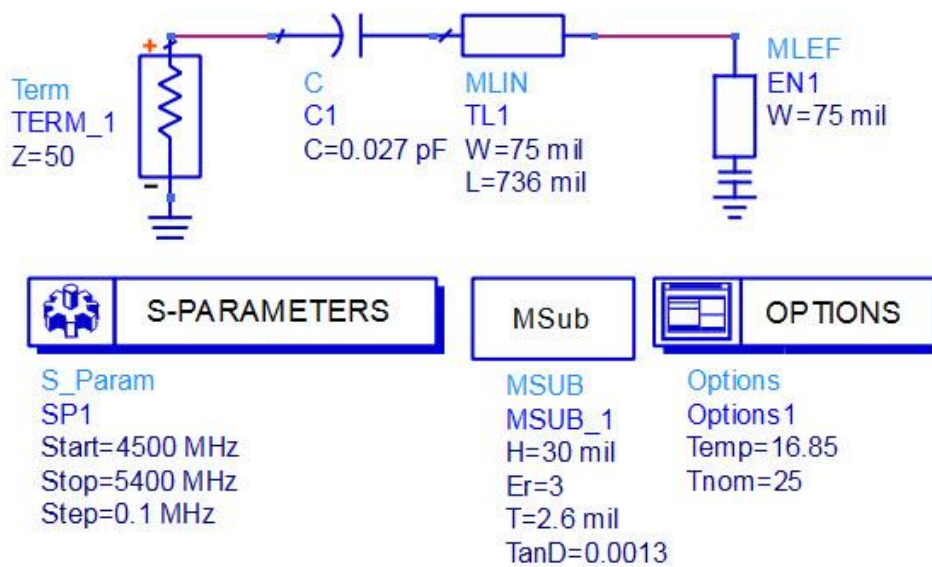


**Figure 4-18** Capacitive coupled half-wave microstrip resonator

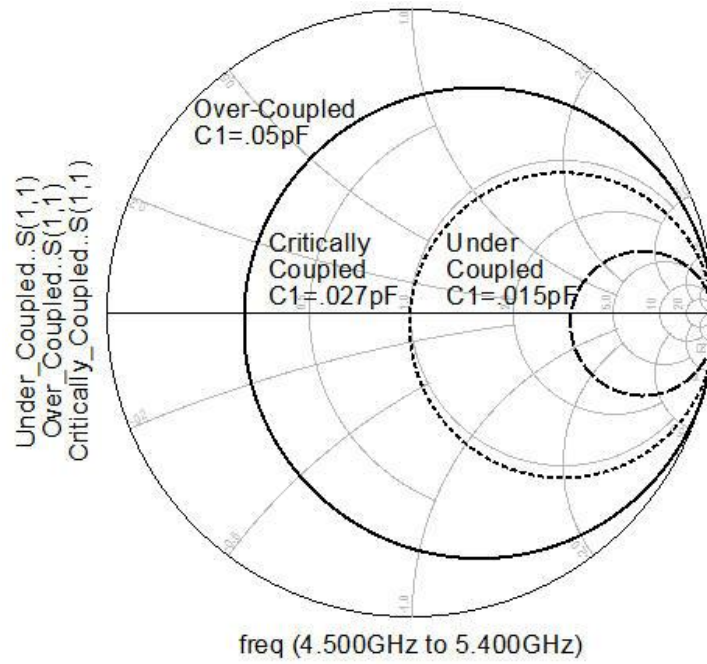


**Figure 4-19** Smith chart plots of the resonator input reflection coefficients

Figure 4-20 shows the scalar plot of the input reflection coefficients.

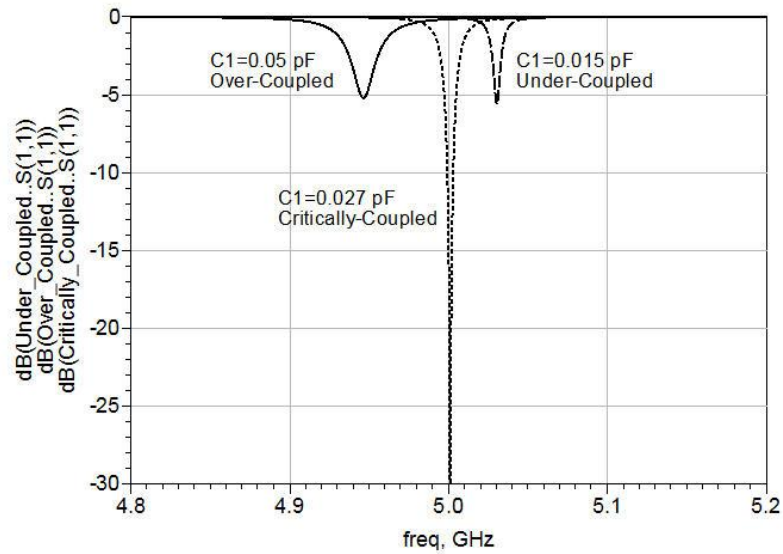


**Figure 4-20** Scalar plots of the resonator input reflection coefficients

### 4.6.1 One Port Microwave Resonator Analysis

The microstrip half wave resonator was fairly easy to model and analyze in ADS. Many microwave resonators are not as easy to model. High Q microwave resonators are often realized as metallic cavities or dielectric resonators. The reactive coupling of the resonator to the circuit can be even more difficult to model. The coupling usually occurs by magnetic or electric coupling by a probe or loop inserted into the cavity. An E field probe coupled to a coaxial cavity resonator is shown in Figure 4-21. A dielectric resonator is coupled to a microstrip line by flux linkage in air as shown in Figure 4-22. The designer is left to develop approximate models based on a lumped RLC equivalent models and couple the resonator to the circuit using an ideal transformer model. Linear simulation can still be of value in the design and evaluation process if we have a measured S parameter file of the resonator's reflection coefficient. Just as we have used S parameter models to represent capacitors and inductors we can also use the measured S parameters of a resonator. All modern vector network analyzers have the ability to save an S parameter data file for any measurement that can be made by the instrument. This section will show how we can use ADS to analyze the S parameter file of a microwave resonator.

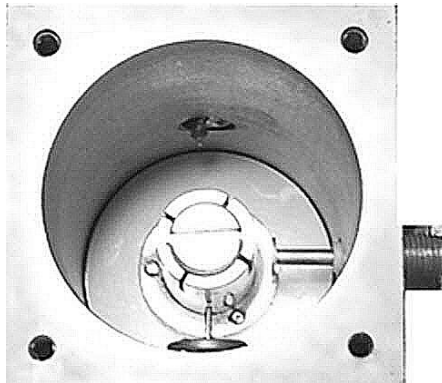


**Figure 4-21** Coaxial cavity with E field probe coupled to center conductor

The coupling of microwave resonators is often characterized by a coupling coefficient  $k$ . The coupling coefficient is the ratio of the power dissipated in the load to the power dissipated in the resonator <sup>[5]</sup>.

$$k = \frac{P_{load}}{P_{resonator}} = \frac{Q_o}{Q_{ext}} \quad (4-27)$$

where:

$Q_o$  is the unloaded Q of the resonator

$Q_{ext}$  is the external Q of the resonator

When  $P_{load}$  is equal to  $P_{resonator}$ ,  $k = 1$  and the critical coupling case exists. Substituting the reciprocal Q factor relationship of Equation (4-10) into Equation (4-27) we can relate the coupling coefficient to the loaded  $Q_L$  and unloaded  $Q_o$  of the resonator.

$$Q_L = \frac{Q_o}{1+k} \quad (4-28)$$



**Figure 4-22** Dielectric resonator coupled to microstrip transmission line

Now the unloaded  $Q_o$  of the resonator can be calculated if the  $Q_L$  and  $k$  can be measured. Because the resonator is a one port device we cannot pass a signal through the device and measure the 3dB bandwidth as was done in section 4.5.3. Kajfez <sup>[5]</sup> has described a technique to extract the coupling coefficient  $k$  and  $Q_L$  values from the Q circle of the resonator. Consider the Q circle on the Smith chart of Figure 4-23. A line that is projected from the center of the Smith chart to intersect the Q circle with minimum length will intersect the circle at the loaded resonance frequency,  $f_L$ . The length of this vector is

labeled as  $|\Gamma_L|$ . As the line projects along a path of the diameter of the circle it intersects the circle near the circumference of the Smith chart at a point defined as  $|\Gamma_d|$ . The input reflection coefficient of the Q circle can be defined using the following empirical equation <sup>[5]</sup>.

$$\Gamma_i = \Gamma_d \left[ 1 - \frac{2k}{1+k} \cdot \frac{1}{1 + jQ_L 2 \frac{\omega - \omega_L}{\omega_o}} \right] \quad (4-29)$$

Lines that are projected from  $\Gamma_d$  through the Q circle at the angles  $\pm\phi$  are related to the loaded Q by Equation (4-30).

$$Q_L = \frac{f_L}{f_1 - f_2} \tan \phi \quad (4-30)$$

If we set  $\phi = 45^\circ$  then Equation (4-30) reduces to the straightforward definition of  $Q_L$  given by Equation (4-31).

$$Q_L = \frac{f_L}{f_1 - f_2} \quad (4-31)$$

In section 2.6 we noticed that the diameter of the circle was directly related to the coupling coefficient. The circle diameter can be measured from:

$$|\Gamma_d| - |\Gamma_L| = d \quad (4-32)$$

The coupling coefficient is then derived from the diameter of the Q circle.

$$k = \frac{d}{2-d} \quad (4-33)$$

Finally the unloaded resonator  $Q_o$  is then calculated from Equation (4-28). We can also find the unloaded resonance frequency directly from the Q circle.

Follow the reactive line on the Smith chart that intersects the Q circle at  $\Gamma_d$  to the next Q circle intersection. The frequency at this Q circle intersection is the unloaded resonance frequency,  $f_o$ .

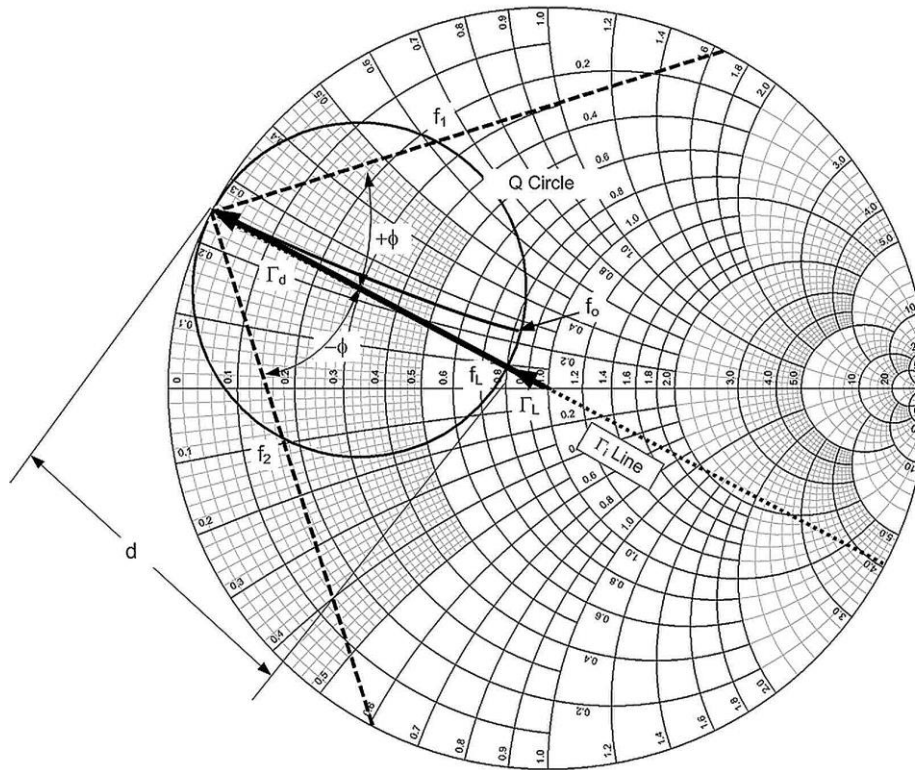


**Figure 4-23** Resonator Q measurement from the resonator Q circle

## 4.7 Filter Design at RF and Microwave Frequency

In Section 4.3 we have seen that it is possible to change the shape of the frequency response of a parallel resonant circuit by choosing different source and load impedance values. Likewise multiple resonators can be coupled to one another and to the source and load to achieve various frequency shaping responses. These networks are referred to as filters.

### 4.7.1 Filter Topology

The subject of filter design is a complex topic and the subject of many dedicated texts <sup>[1,2]</sup>. This section is intended to serve as a fundamental primer

to this vast topic. It is also intended to set a foundation for successful filter design using the ADS software. The four most popular filter types are: Low Pass, High Pass, Band Pass, and Band Stop. The basic transmission response of the filter types is shown in Figure 4-24A and 4-24B. The filters allow RF energy to pass through their designed pass band. RF energy that is present outside of the pass band is reflected back toward the source and not transmitted to the load. The amount of energy present at the load is defined by the  $S_{21}$  response. The amount of energy reflected back to the source is characterized by the  $S_{11}$  response.

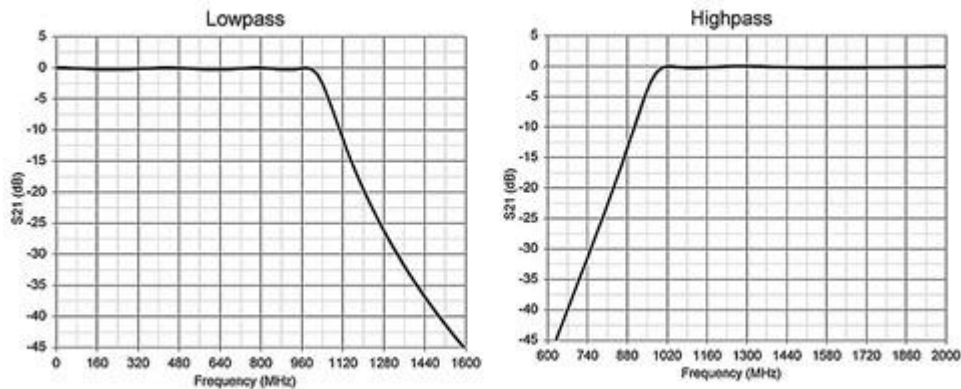


Figure 4-24A  $S_{21}$  versus frequency characteristic for the basic filter types

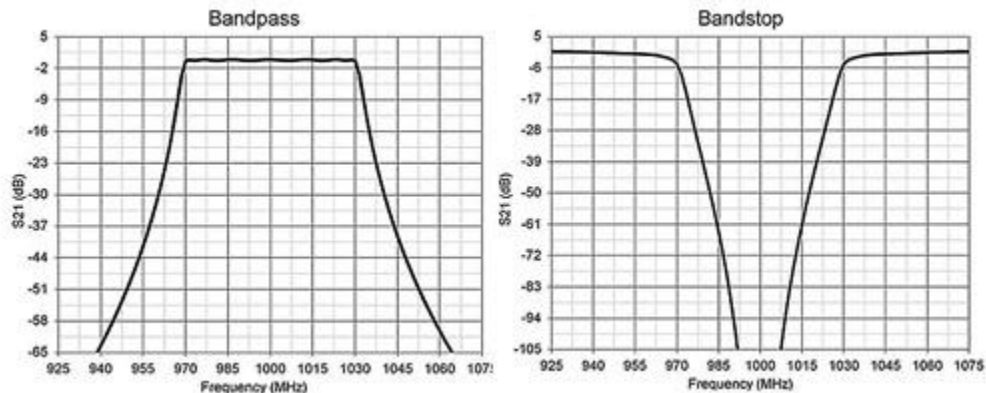


Figure 4-24B  $S_{21}$  versus frequency characteristic for the basic filter types



### 4.7.2 Filter Order

The design process for all of the major filter types is based on determination of the filter pass band, and the attenuation in the reject band. The attenuation in the reject band that is required by a filter largely determines the slope needed in the transmission frequency response. The slope of the filter's response is related to the order of the filter. The steeper the slope or 'skirt' of the filter; the higher is the order. The term order comes from the mathematical transfer function that describes a particular filter. The highest power of  $s$  in the denominator of the filter's Laplace transfer function is the order of the filter. For the simple low pass and high pass filters presented in this chapter the filter order is the same as the number of elements in the filter. However this is not the case for general filter networks. In more complex types of lowpass and highpass filters as well as bandpass and bandstop filters the filter order will not be equal to the number of elements in the filter. In the general case the filter order is the total of the number of transmission zeros at frequencies:

- $F = 0$  (DC)
- $F = \infty$
- $0 < F < \infty$  (specific frequencies between DC and  $\infty$ )

Transmission zeros block the transfer of energy from the source to the load. In fact the order of a filter network can be solved visually by adding up the number of transmission zeros that satisfy the above criteria. Figure 4-25 shows the relationship between the filter order and slope of the response for a Low Pass filter. Each filter of Figure 4-26 has the same cutoff frequency of 1000 MHz. The third order filter has an attenuation of about 16 dB at a rejection frequency of 2000 MHz. The fifth order filter shows an attenuation of 39 dB and the seventh order filter has more than 61 dB attenuation at 2000 MHz. It is therefore clear that the order of the filter is one of the first criteria to be determined in the filter design. It is dependent on the cutoff frequency of the pass band and the amount of attenuation desired at the rejection frequency.

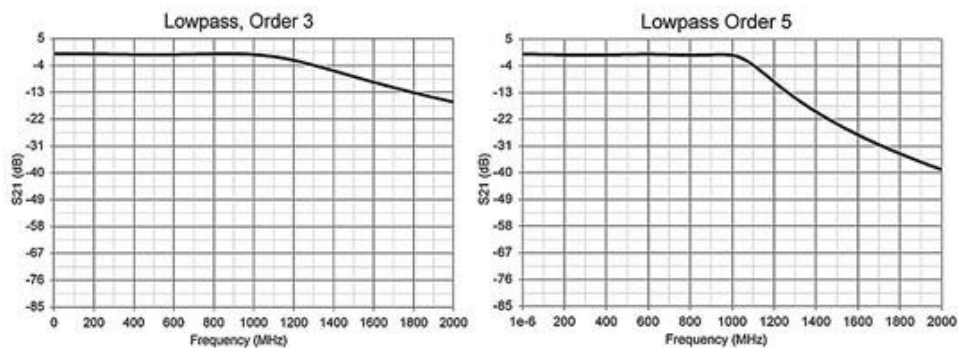


**Figure 4-25A** Relationship between filter order and the slope of S21

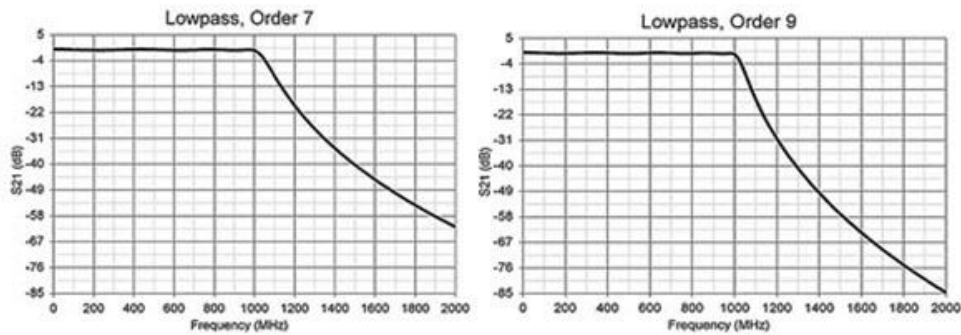


**Figure 4-25B** Relationship between filter order and the slope of S21

### 4.7.3 Filter Type

The shape of the filter passband and attenuation skirt can take on different shape relationships based on the coupling among the various reactive elements in the filter. Over the years several polynomial expressions have been developed for these shape relationships. Named after their inventors, some of the more popular types include: Bessel, Butterworth, Chebyshev, and Cauer. Figure 4-26 shows the general shape relationship among these filter types. The Bessel filter is a low Q filter and does not exhibit a steep roll off. The benefit of the Bessel filter is its linear phase or flat group delay response. This means that the Bessel filter can pass wideband signals while introducing little distortion. The Butterworth is a medium Q filter that has the flattest pass band of the group. The Chebyshev response is a higher Q filter and has a noticeably steeper skirt moving toward the reject band.

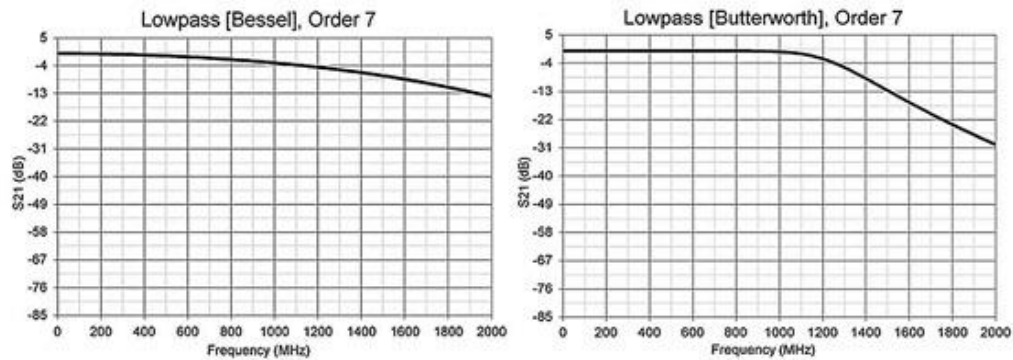


**Figure 4-26 A** shape of Bessel and Butterworth filters

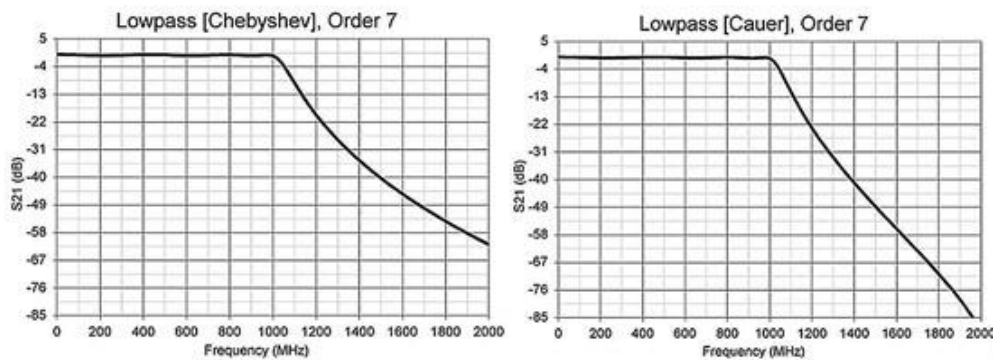


**Figure 4-26 B** shape of Chebyshev, and Cauer filters

As a result it exhibits more transmission ripple in the pass band. The Cauer filter has the steepest slope of all of the four filter types. The Cauer filter is also known as an elliptic filter. Odd order Chebyshev and Cauer filters can be designed to have an equal source and load impedance. The even order Chebyshev and Cauer filters will have different output impedance from the specified input impedance. Another interesting characteristic of the Cauer filter is that it has the same ripple in the rejection band as it has in the pass band. The Butterworth, Chebyshev and Cauer filters differ from the Bessel filter in their phase response. The phase response is very nonlinear across the pass band. This nonlinearity of the phase creates a varying group delay. The group delay introduces varying time delays to wideband signals which, in turn, can cause distortion to the signal. Group delay is simply the derivative, or slope, of the transmission phase and defined by Equation (4-34). Figure 4-27 shows the respective set of filter transmission characteristics with their

corresponding group delay. Note the relative values of the group delay on the right hand axis.

$$\tau_g = -\frac{d\phi}{d\omega} \quad (4-34)$$

where,  $\phi$  is phase shift in radians and  $\omega$  is frequency in radians per second.

From the group delay plots of Figures 4-27 it is evident that the group delay peaks near the corner frequency of the filter response. The sharper cutoff characteristic results in greater group delay at the band edge.

#### **4.7.4 Filter Return Loss and Passband Ripple**

The Bessel and Butterworth filters have a smooth transition between their cutoff frequency and rejection frequency. The forward transmission, S<sub>21</sub>, is very flat vs. frequency. The Chebyshev and Cauer filters have a more abrupt transition between their cutoff and rejection frequencies. This makes these filter types very popular for many filter applications encountered in RF and microwave engineering. It is also clear from Figure 4-27 that a sharp-cutoff response is generally incompatible with a good phase response or group delay in the passband region <sup>[6]</sup>.

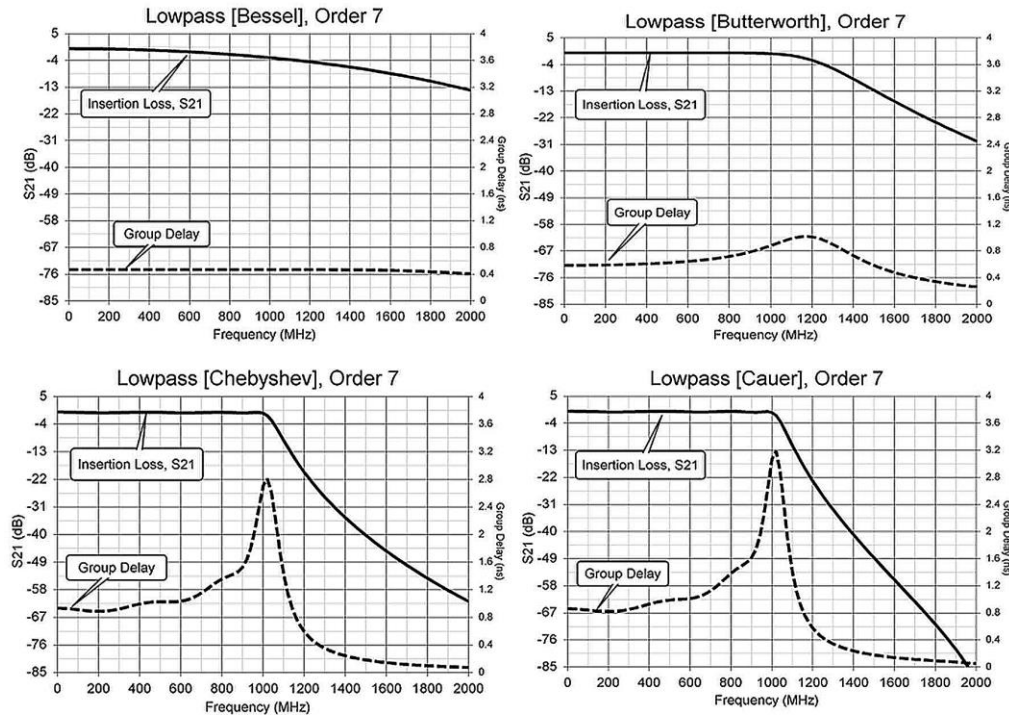


**Figure 4-27** Group delay characteristic for various lowpass filter types

The Chebyshev and Cauer filter types have ripple in the forward transmission path,  $S_{21}$ . The amount of ripple is caused by the degree of mismatch between the source and load impedance and thus the resulting return loss that is realized by these filter types. For a given Chebyshev or Cauer filter order, the roll off of the filter response is also steeper for greater values of passband ripple. The cutoff frequency of the filters that have passband ripple is then defined as the passband ripple value. For all-pole filters such as the Butterworth, the cutoff frequency is typically defined as the 3 dB rejection point. Figure 4-28 shows the passband ripple of a fifth order low pass filter for ripple values of 0.01, 0.1, 0.25, and 0.5 dB. Note that the ripple shown is produced by ideal circuit elements. In practice the finite unloaded  $Q$  or losses in the inductors and capacitors will tend to smooth out this ripple.

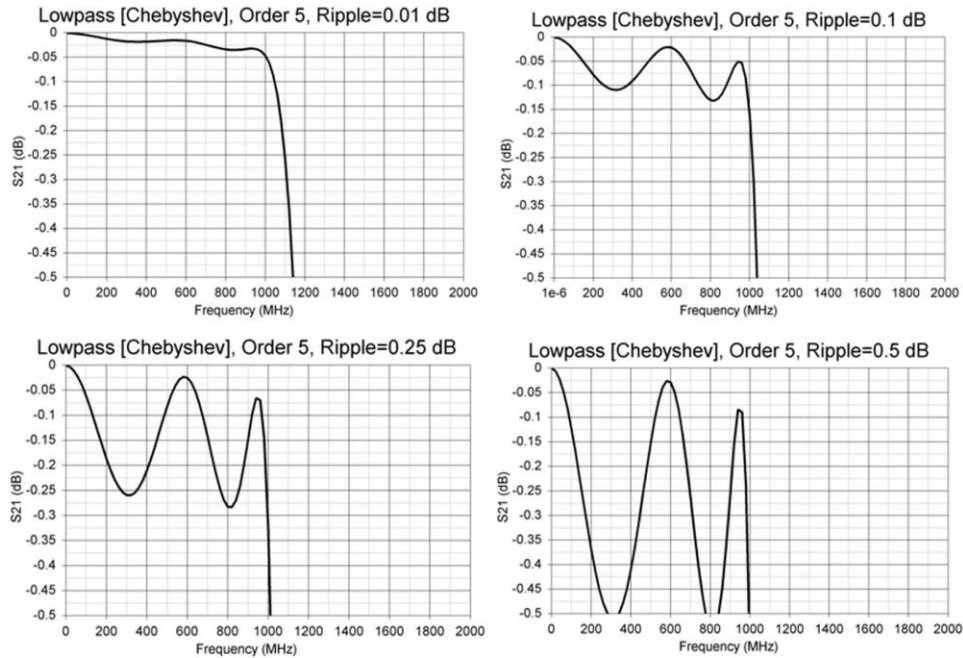


**Figure 4-28** Passband ripple values in lowpass Chebyshev filter

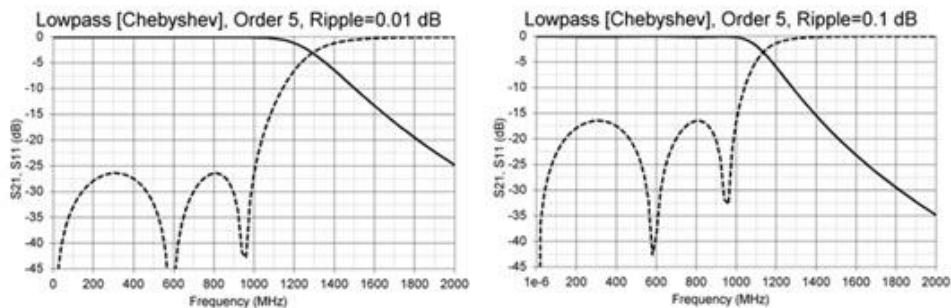
In Chapter 2 the relationship for mismatch loss between a source and load was presented. For the Chebyshev and Cauer filters this mismatch loss is the passband ripple.

vswr ( )	ReturnLoss_dB ( )	Ripple_dB ( )
1.1	26.444	0.01
1.239	19.433	0.05
1.3	17.692	0.075
1.355	16.435	0.1
1.405	15.473	0.125
1.452	14.688	0.15
1.538	13.474	0.2
1.62	12.518	0.25
1.984	9.636	0.5

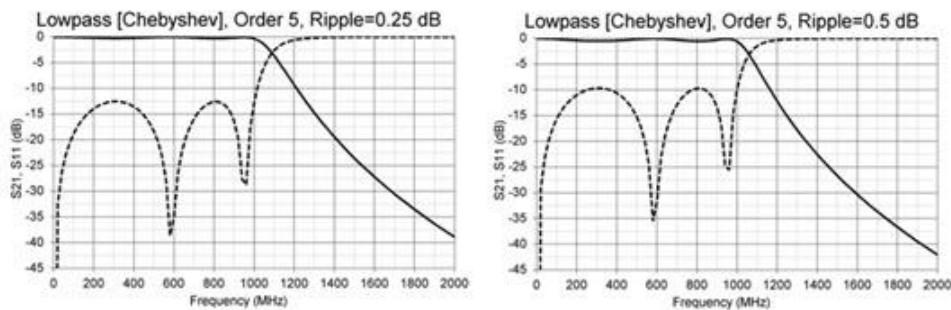
**Figure 4-29** Calculation of filter ripple versus VSWR

Figure 4-30 shows the same filters from Figure 4-28 with the return loss plotted along with the insertion loss,  $S_{21}$ . We can see that for a given filter

order, there is a tradeoff between filter rejection and the amount of ripple, or return loss, that can be tolerated in the passband. In most RF and microwave filter designs the 0.01 and 0.1 dB ripple values tend to be more popular. This is due to the tradeoff between good impedance match and reasonable filter skirt slope. Figure 4-28 shows good correlation of the worst case return loss with that which is calculated in Figure 4-29. When tuning filters using modern network analyzers it is sometimes easier to see the larger changes in the return loss as opposed to the fine grain ripple as shown in Figure 4-28. For this reason it is common to tune the forward transmission of the filter by observing the level and response of the filter's return loss. Return loss is a very sensitive indicator of the filter's alignment and performance.



**Figure 4-30A** Lowpass Chebyshev filter rejection and return loss versus passband ripple



**Figure 4-30B** Lowpass Chebyshev filter rejection and return loss versus passband ripple

## 4.8 Lumped Element Filter Design

Classical filter design is based on extracting a prototype frequency-normalized model from a myriad of tables for every filter type and order.

Fortunately these tables have been built into many filter synthesis software applications that are readily available. In this book we will examine the filter synthesis tool that is built into the ADS software. We will work through two practical filter examples, one low pass and one high pass using the ADS filter synthesis tool.

### 4.8.1 Low Pass Filter Design Example

As a practical filter design, consider a full duplex communication link (simultaneous reception and transmission) through a satellite with the following requirements:

- The uplink signal is around 145 MHz while the downlink is at 435 MHz.
- A 20 W power amplifier is used on the uplink with 25 dB gain.
- It is necessary to provide a low pass filter on the uplink (only pass the 145 MHz uplink signal while rejecting any noise power in the 435 MHz band).
- It is necessary to provide a high pass filter on the downlink so that the 435 MHz downlink signal is received while rejecting any noise at 145 MHz.

The transmitter and receiver antennas are on the same physical support boom so there is limited isolation between the transmitter and receiver. Even though the signals are at different frequencies, the broadband noise amplified by the power amplifier at 435 MHz will be received by the UHF antenna and sent to the sensitive receiver. Because the receiver is trying to detect very low signal levels, the received noise from the amplifier will interfere or ‘de-sense’ the received signals.

**Example 4.8-1:** Design a 145 MHz Low Pass filter for this satellite link system with the following specifications.

- Having a Chebyshev Response with 0.1 dB pass band ripple.
- Having a passband cutoff frequency (not the -3 dB frequency) at 160 MHz
- Having at least -40 dB rejections at 435 MHz.

**Solution:** Create a new workspace, EX4.8-1\_wrk, and a new schematic in cell\_1. Follow the procedure below to design the low pass filter.



- From the schematic window, click DesignGuide > Filter > Filter Control Window to open the Filter DesignGuide Control Window, as shown in Figure 4-31.

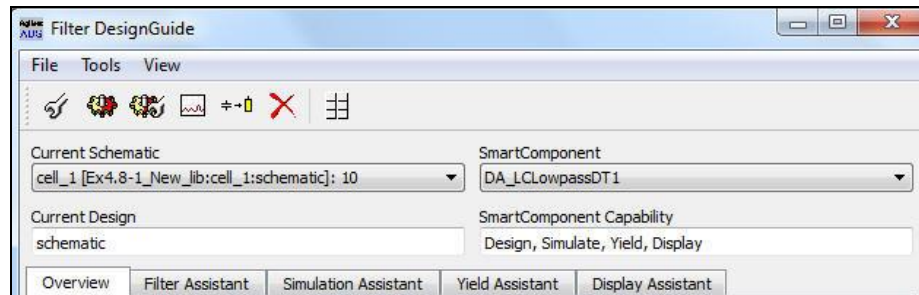


**Figure 4-31** Filter DesignGuide control window

- In the Filter DesignGuide Control Window, click View > Component Palette-All to place the SmartComponent Palettes in the schematic window.
- From the list of Filter DG - All Palette in the schematic window, select the lowpass filter SmartComponent, DA\_LCLowpassDT.

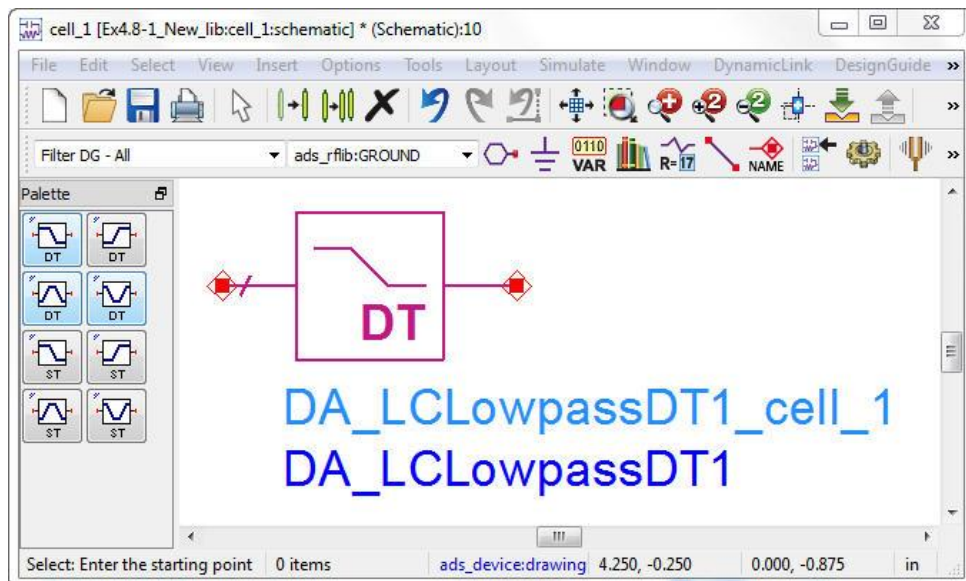


**Figure 4-32** SmartComponent Palette in the schematic window

- Click anywhere within the schematic window to place the component.
- Double-click the SmartComponent to open a dialog box containing all parameters.
- Modify the parameters to meet the design specifications, as shown in Figure 4-33.

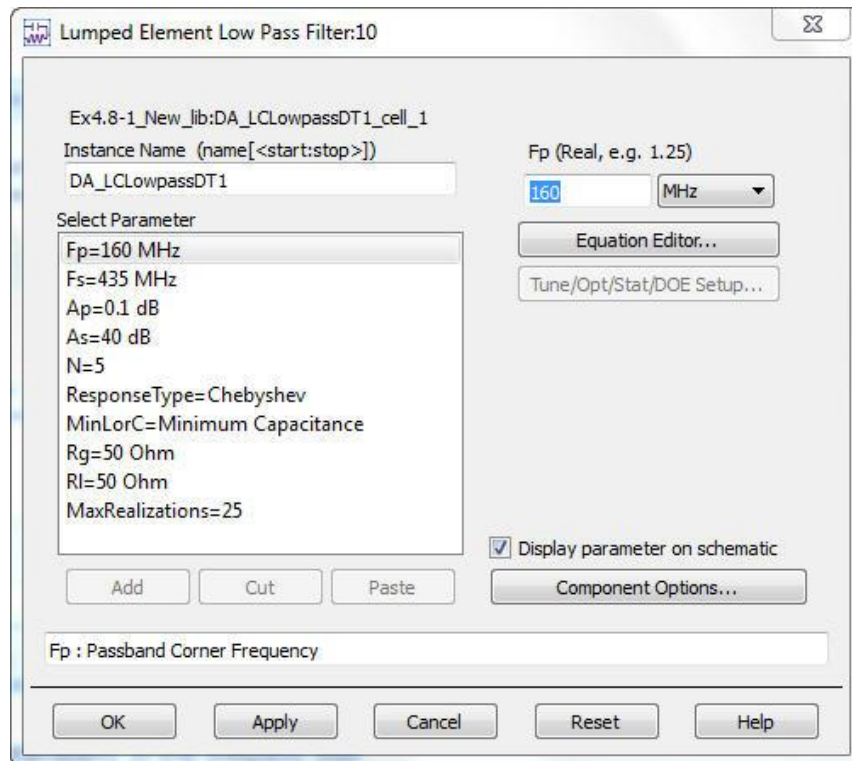


**Figure 4-33** Modified parameters of the lowpass filter

- In the Filter DesignGuide control window select the Filter Assistant tab and click Design to start a simulation and generate the filter sub-network, as shown in Figure 4-34.

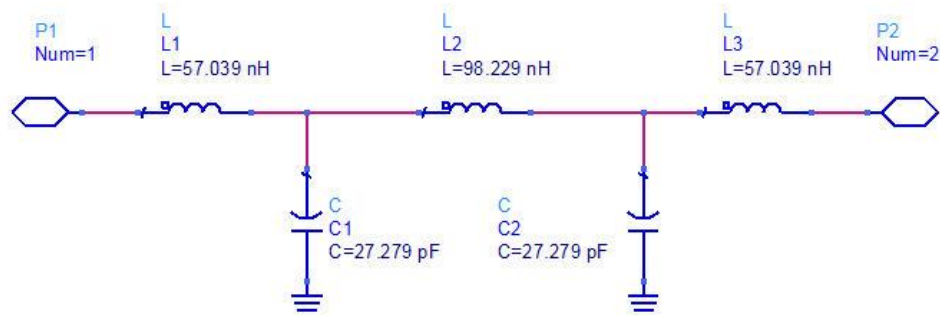


**Figure 4-34** Lowpass filter sub-network (N=5)

The required filter order is determined by increasing the order until the specification of -40 dBc attenuation at 435 MHz is achieved. As the filter response curve in Fig.4-36 shows, this Low Pass filter must be of fifth order to achieve the required attenuation.

After SmartComponents are designed and tested, they can be used as standalone components. The Filter DesignGuide is not needed to use them in new designs unless you want to modify or analyze them. In Figure 4-35 the lowpass filter SmartComponent is used in S parameter simulation circuit.

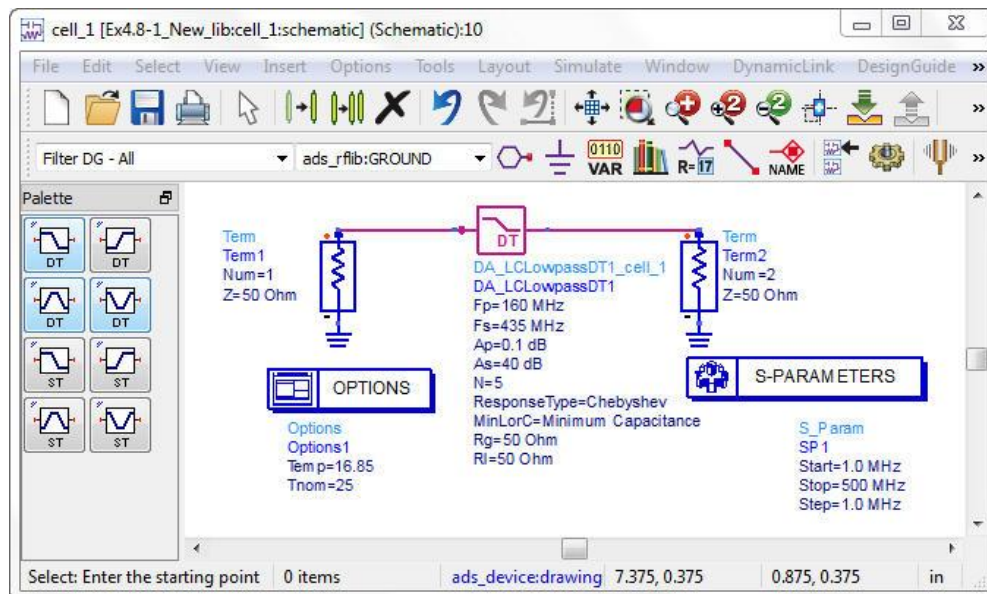


**Figure 4-35** SmartComponent used in S parameter simulation circuit

Simulated Response of the low pass filter is shown in Figure 4-36.

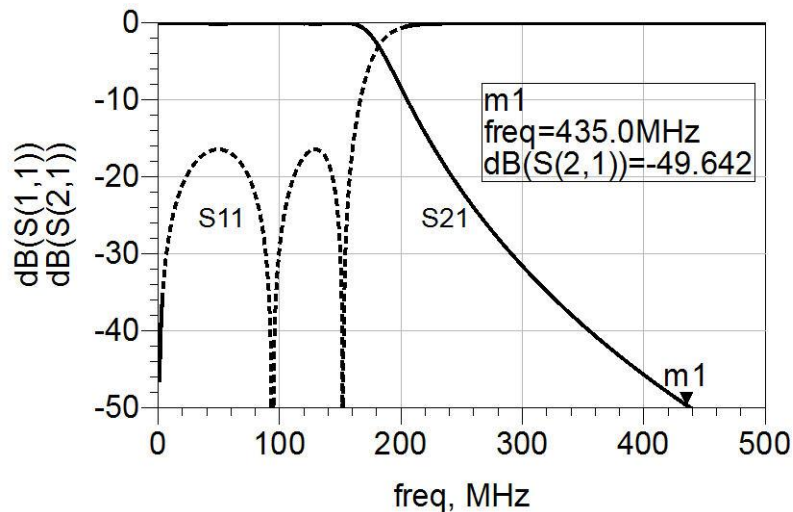


Figure 4-36 Simulated Response of the low pass filter

#### 4.8.2 Physical Model of the Low Pass Filter in ADS

It is important to realize that the synthesized filter is an ideal design in the sense that ideal (no parasitics and near infinite  $Q$ ) components have been used. To obtain a good ‘real-world’ simulation of the filter we need to use component models that have finite  $Q$  and parasitics such as multilayer chip capacitors for shunt capacitors. For the capacitors, choose the 6003 series chip capacitors from ATC Corporation. ATC Corporation has a useful application for selection of chip capacitors called ATC Tech Select. This program is available for free download from the ATC web site: [www.atceramics.com](http://www.atceramics.com). ATC also provides S-Parameter files for their capacitors that are readily available on the company website. For the physical design of the filter in Figure 4-37 the ATC capacitor models must be installed into the ADS workspace.

Because the filter is passing relatively high power (20 W), we cannot use small surface mount style chip inductors. Instead we will use air wound coils to realize the series inductors. The inductors will be realized with AWG#16 wire nickel-tin plated copper wire. The wire has a diameter of 0.05 inches or 50 mils. They will be wound on a 0.141 inch diameter form. Use the

techniques covered in Chapter one, Section 1.4.1 to design the air-core wound inductors. The filter model is then reconstructed using the physical inductor models for the series inductors. Make sure to model the substrate and the interconnecting printed circuit board traces as microstrip lines. Also model the ground connection of the shunt capacitors as a microstrip via hole.

Although these PCB parasitic effects are normally more pronounced at frequencies above 2 GHz, it is often surprising the effect that these parasitics have at lower frequencies. The physical filter schematic is shown in Figure 4-37.

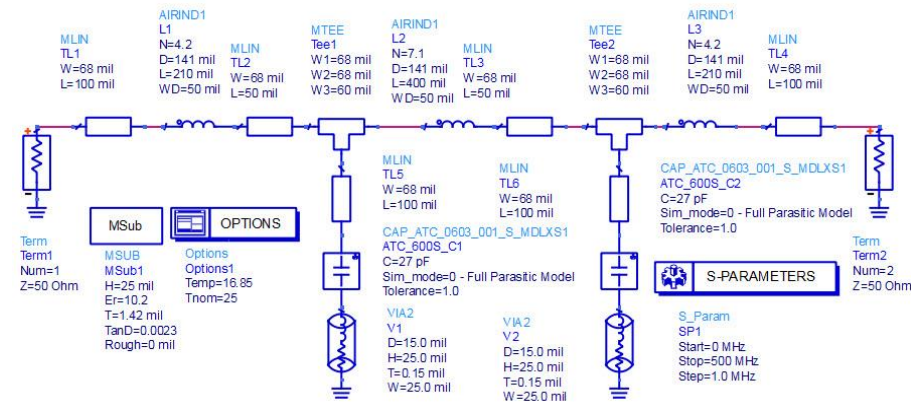


**Figure 4-37** Schematic of the physical low pass filter

The physical filter response is shown in Figure 4-38.

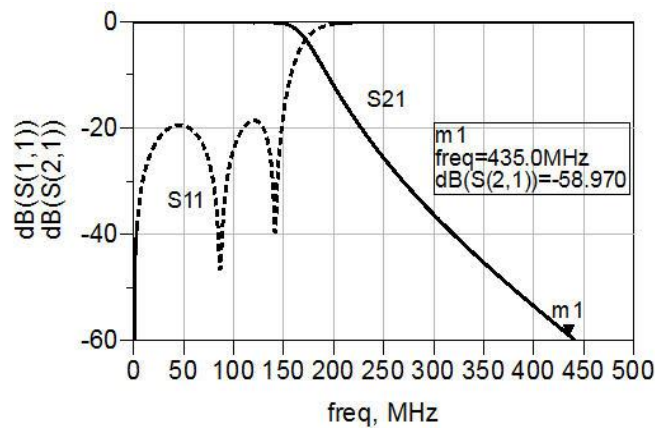


**Figure 4-38** Response of the physical lowpass filter

The response shows that the attenuation specification at 435 MHz has been achieved. Because the circuit has physical models replacing the ideal lumped elements, the engineer is reasonably confident that the filter can be assembled and will achieve the designed response. In section 4.9 the lumped element filters are transformed to microstrip line filters with layouts for EM simulation.

Figure 4-39 is a photo of the prototype low pass filter circuit with SMA coaxial connectors attached to the circuit board.

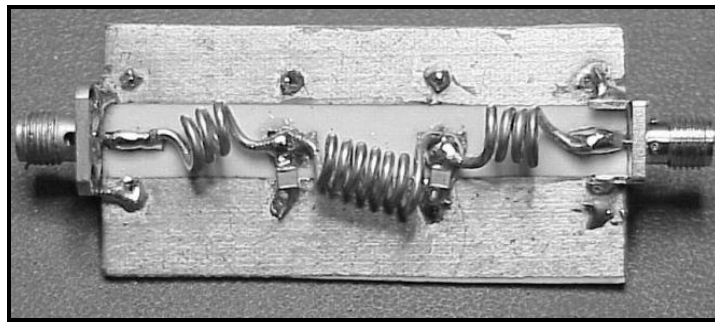


**Figure 4-39** Physical prototype of the low pass filter (courtesy of BT Microwave LLC)

### 4.8.3 High Pass Filter Design Example

**Example 4.8-2:** Design a high pass filter that passes frequencies in the 420 MHz to 450 MHz range. This filter could be placed in front of the preamp used in the downlink of the satellite system. This would help to keep out any of the transmit energy or noise power in the 146 MHz transmit frequency range. The High Pass Filter specifications are:

- The pass band cutoff frequency (not the -3 dB frequency) is 420 MHz.
- The filter has a Chebyshev response with 0.1 dB pass band ripple.
- The reject requirement is at least -60 dB rejections at 146 MHz.

**Solution:** Following the procedure in Example 4.8.1 create a new workspace in ADS and open a new schematic window. From the schematic window, click DesignGuide > Filter > Filter Control Window to open the Filter DesignGuide control window. In the Filter DesignGuide control window, click View > Component Palette-All to place the filter SmartComponent

Palette in the schematic window. From the list of Filter DG-All Palette select the highpass filter SmartComponent, DA\_LCHighpassDT, and click anywhere within the schematic window to place the component. Modify the component parameters to meet the highpass filter design specifications, as shown in Figure 4-40.

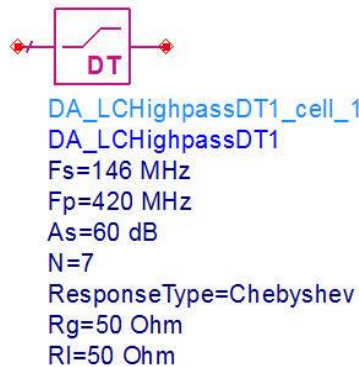


**Figure 4-40** Parameters of the highpass filter

The required filter order is determined by increasing  $N$  until the specification of  $-60$  dBc attenuation at  $146$  MHz is achieved. It is always a good practice to design for some additional rejection (margin) that exceeds the minimum requirement, as shown in Figure 4-41. The Filter DesignGuide session recommends a filter of  $7^{\text{th}}$  order.

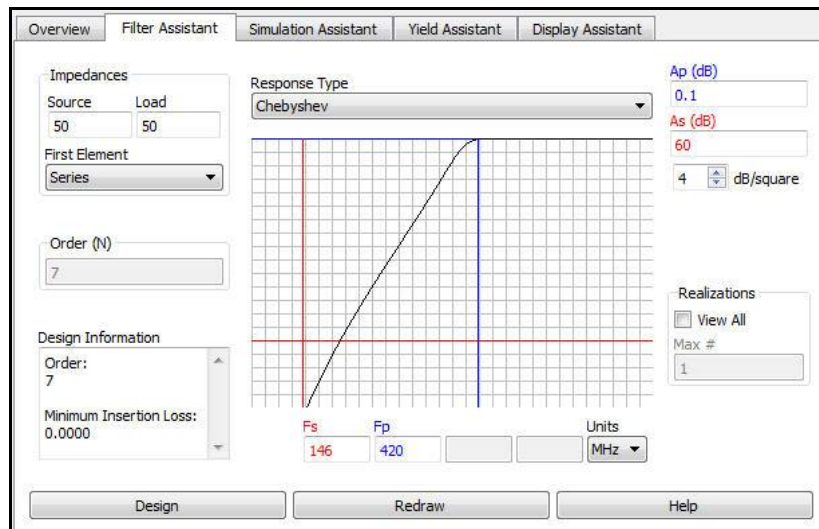


**Figure 4-41** DesignGuide highpass filter response

The high pass filter sub-network is shown in Figure 4-42.

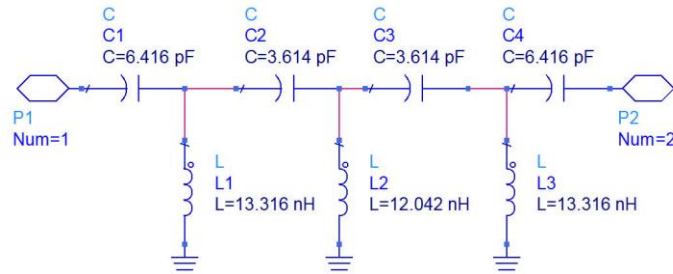


**Figure 4-42** Lumped element model of the high pass filter (N=7)

Attach 50 Ohm terminations to the highpass filter SmartComponent model and simulate the schematic from 100 to 500 MHz, as shown in Figure 4-43.

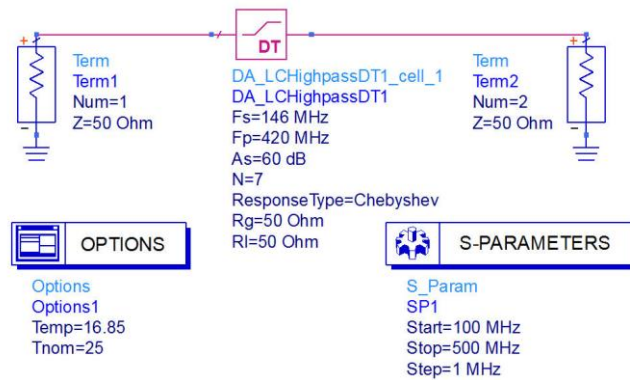


**Figure 4-43** Simulation of the high pass filter

The simulated response of the highpass filter is shown in Figure 4-44.

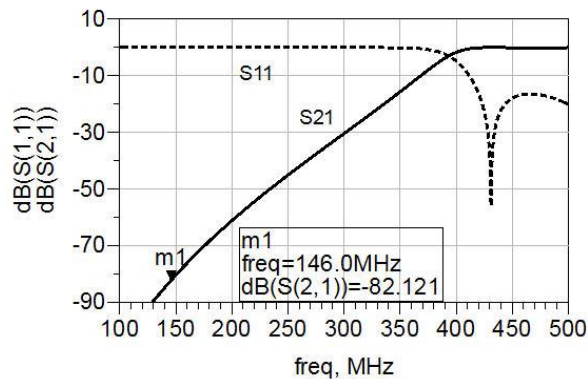


**Figure 4-44** Response of the high pass filter



As Figure 4-44 shows the attenuation of -60 dBc at 146 MHz has been achieved with a good margin.

#### 4.8.4 Physical Model of the High Pass Filter in ADS

Using the same techniques as described for the Low Pass Filter design we can proceed with the High Pass Filter realization. The Filter DesignGuide application calculated series capacitance values of 6.416 pF and 3.614 pF. Looking through the available ATC 700B series chip capacitors, the nearest values are 6.8 pF and 3.9 pF capacitors. The shunt inductors are realized using the Air Wound inductor models. Figure 4-45 shows the completed assembly of the High Pass Filter on a printed circuit board with coaxial SMA connectors.

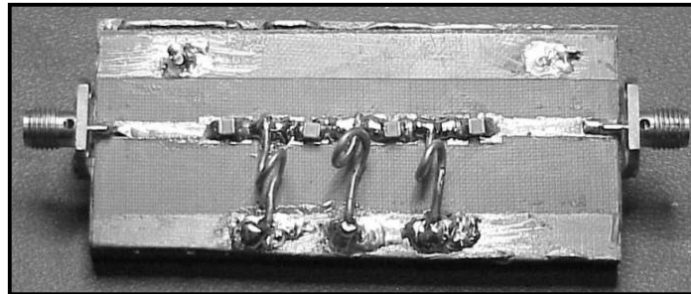


**Figure 4-45** Physical prototype of the 420 MHz highpass filter (courtesy of BT Microwave LLC)

### 4.9 Distributed Filter Design

#### 4.9.1 Microstrip Stepped Impedance Low Pass Filter Design

In the microwave frequency region filters can be designed using distributed transmission lines. Series inductors and shunt capacitors can be realized with microstrip transmission lines. In the next section we will explore the conversion of a lumped element low pass filter to a design that is realized entirely in microstrip.

**Example 4.9-1:** Design a lumped element 2.2 GHz Chebyshev-response lowpass filter having 0.1 dB passband ripple and -40 dB rejection at 6 GHz. Convert all the lumped elements to microstrip transmission lines. The microstrip substrate is Rogers's 6010 material ( $\epsilon_r=10.2$ ) with a 0.025 inch dielectric thickness.

**Solution:** Following the procedure discussed in Example 4.8-1, the SmartComponent design of the lowpass filter is shown in Figure 4-46.

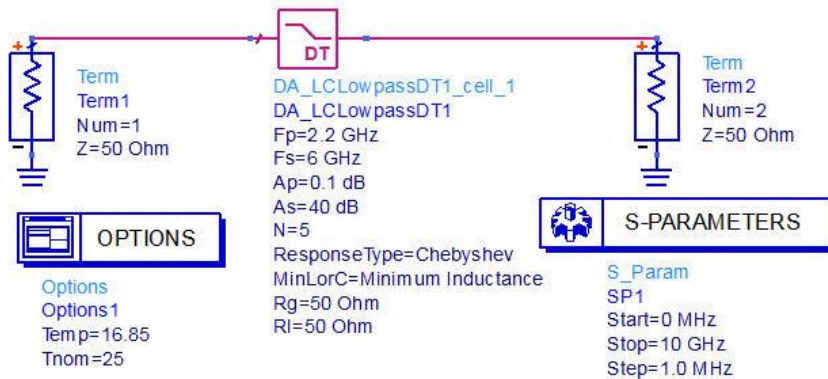


**Figure 4-46** Lumped element design of the 2.2 GHz low pass filter

The lumped element sub-network of the filter is shown in Figure 4-47.

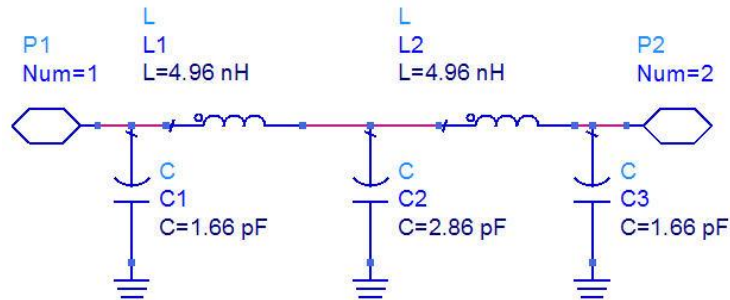


**Figure 4-47** Lumped element 2.2 GHz low pass filter

The simulated response of the filter is shown in Figure 4-48.

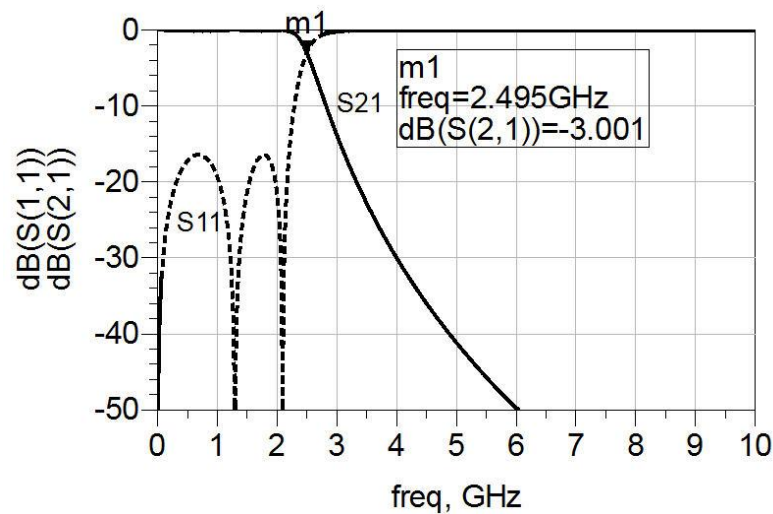


**Figure 4-48** Response of the lumped element 2.2 GHz lowpass filter

The marker m1 in Figure 4-48 shows that the 3 dB bandwidth of the lowpass filter is 2495 MHz.

### 4.9.2 Lumped Element to Distributed Element Conversion

After a Filter DesignGuide SmartComponent has been designed, the lumped inductors and capacitors can be transformed into equivalent distributed element counterparts using the ADS Transformation Assistant. The Filter Transformation Assistant helps us to quickly and easily transform an ideal filter topology to a form that is realizable for RF and microwave systems.

The Transformation Assistant is opened from the Filter DesignGuide Control window, by selecting Tools > Distributed Element Transformations. When the Transformation Assistant is opened, the SmartComponent subnetwork appears in the schematic window and a dialog box is opened. The transformations are then accomplished using the controls on the dialog box.

After the Transformation Assistant has been selected, the graphical area displays the components that can be transformed. Black components represent elements included in the original circuit available for transformation, while gray components represent elements not included in the original circuit.

Check the LC, TLine to Microstrip transformations and select the series inductors L1 and L2 to be transformed to microstrip transmission lines.

Set the characteristic impedance of the microstrip line to  $Z_0 = 80$  Ohm and enter the microstrip substrate parameters, as shown in Figure 4-49.

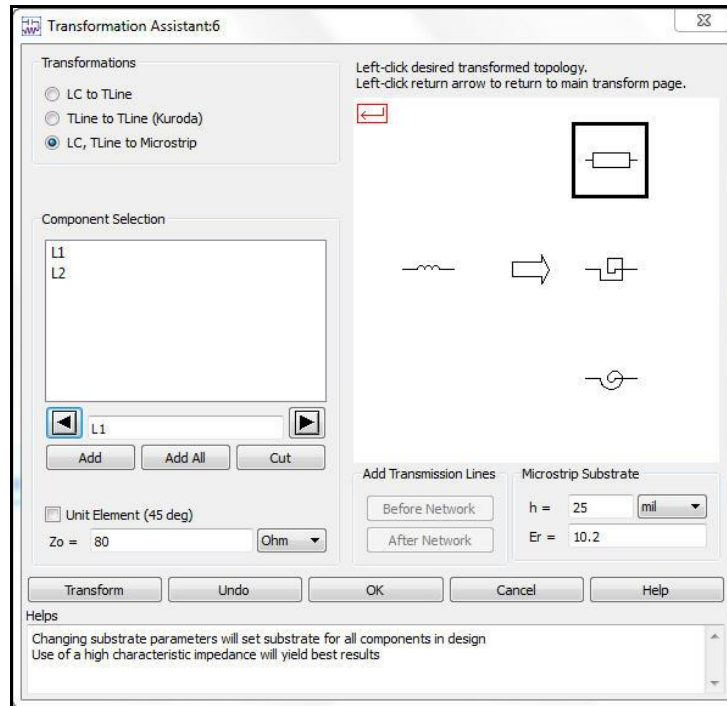


**Figure 4-49** Transformation Assistance window

Click Transform and then click OK. As Figure 4-50 shows the series inductors L1 and L2 have been transformed to  $80 \Omega$  microstrip transmission lines on the microstrip substrate.

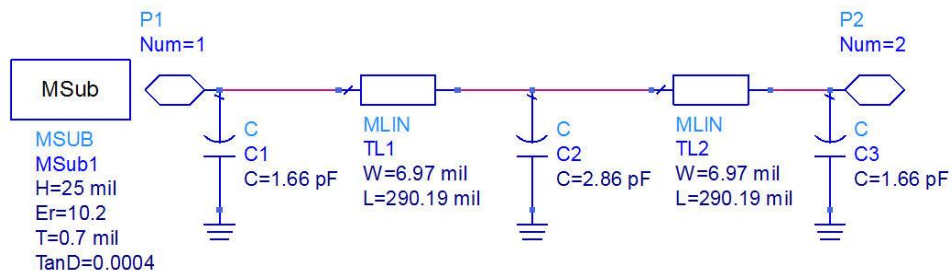


**Figure 4-50** Series inductors transformed to microstrip lines

From the graphical area, use the left red arrow to select the shunt capacitors for transformation. The graphical area changes to reveal the other distributed element equivalents available for substitution. Repeat the same process for the capacitors but select  $Z_0 = 20$  Ohm, as shown in Figure 4-51.

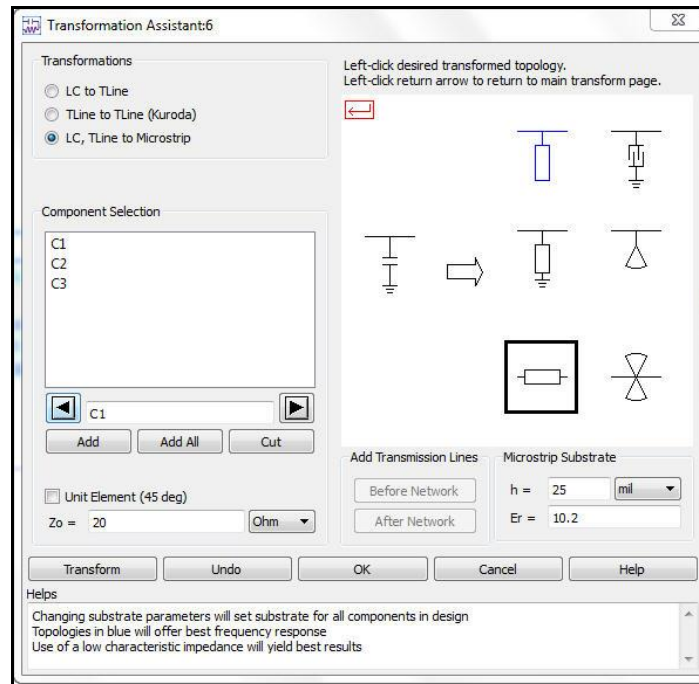


**Figure 4-51** Transformation of shunt capacitors to 20  $\Omega$  microstrip line

Click Transform and then click OK. Now the capacitors have also been transformed to microstrip lines.

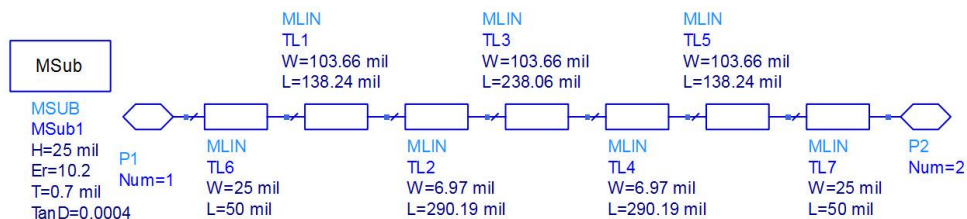


**Figure 4-52** Initial schematic of the distributed low pass filter

Now the lumped element filter in Figure 4-47 has been converted to microstrip stepped impedance low pass filter of Figure 4-52. Simulate the schematic in Figure 4-46 and display the response from 0 to 10 GHz.

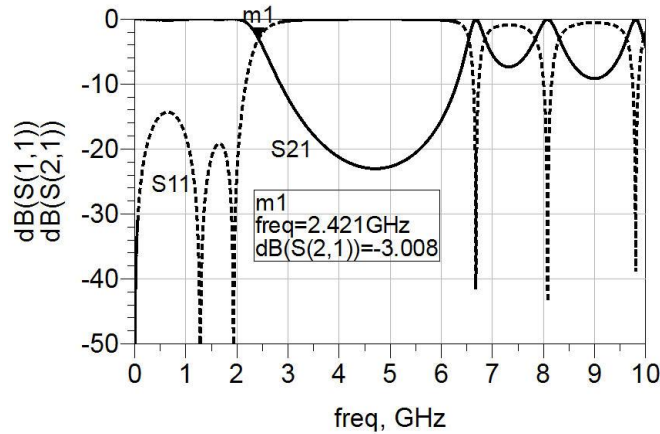


**Figure 4-53** Initial response of the low pass filter

Note that the marker m1 in Figure 4-53 shows that the 3 dB bandwidth of the lowpass filter has slightly decreased to 2421 MHz.

The printed circuit board layout of the initial lowpass filter is shown in Figure 4-54.

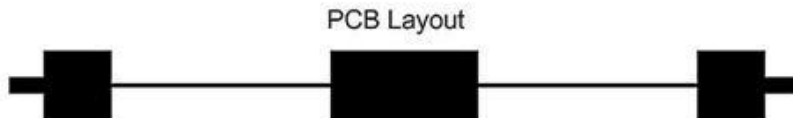


**Figure 4-54** Initial PCB layout of the lowpass filter

Examine the printed circuit board, PCB, layout of the lowpass filter of Figure 4-54. Note the change in geometry as the impedance transitions from  $50\ \Omega$  at the input to  $20\ \Omega$ , representing the shunt capacitor, and then from  $20\ \Omega$  to  $80\ \Omega$ , representing the series inductor. These abrupt changes in geometry are known as discontinuities. Discontinuities in geometry result in fringing capacitance and parasitic inductance that will modify the frequency response of the circuit. At RF and lower microwave frequencies (up to about 2 GHz)

the effects of discontinuities are minimal and sometimes neglected [4]. As the operation frequency increases, the effects of discontinuities can significantly alter the performance of a microstrip circuit. ADS software has several model elements that can help to account for the effects of discontinuities. These include: T-junctions, cross junctions, open circuit end effects, coupling gaps, and bends.

A Microstrip Step element can be placed between series lines of abruptly changing geometry to account for the step discontinuity. Place the Microstrip Step element at each impedance transition in the filter. Make sure that the narrow side and wide side are directed appropriately. The Microstrip Step element, MSTEP, will automatically use the adjacent width in its calculation. Figure 4-55 shows the lowpass stepped impedance filter with the step elements added between each transmission line section.

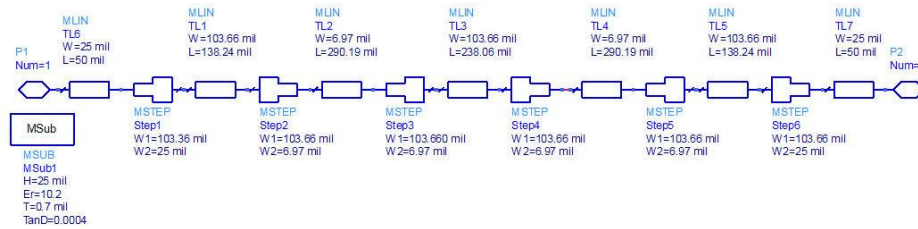


**Figure 4-55** Stepped impedance filter with added “step” elements

The simulated response of the modified filter is shown in Figure 4-56.

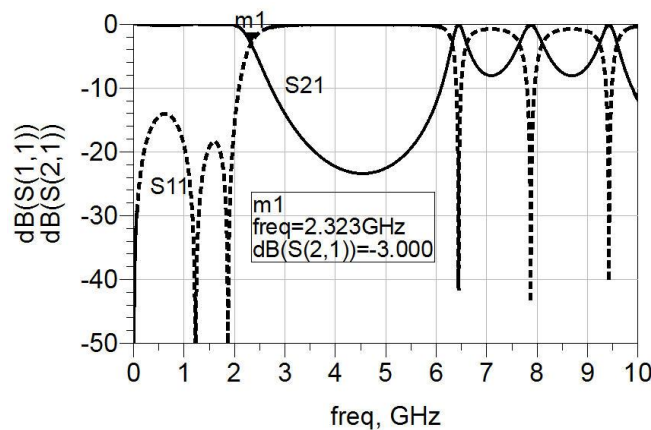


**Figure 4-56** Filter frequency shift due to step discontinuities

A comparison of the initial lowpass filter model response in Figure 4-53 and the modified model response in Figure 4-56 shows that there is some frequency shift in the filter response as it is evidenced, about 100 MHz, by the 3 dB bandwidth.

### **4.9.3 Electromagnetic Analysis of the Stepped Impedance Filter**

Electromagnetic, EM, modeling is a useful tool in microstrip circuit design as it offers a means of potentially more accurate simulation than linear modeling. The linear microstrip component models used to model the stepped impedance filter are based on closed form expressions developed over many years. For many designs the linear model is quite acceptable. Microstrip circuits that contain several distributed components in a dense printed circuit layout will be affected by cross coupling and enclosure effects. This is because the microstrip circuitry is quasi-TEM with some portion of the EM fields in the free-space above the dielectric material. These effects are very difficult to accurately simulate with linear modeling techniques. The ADS software suite has a very useful electromagnetic (EM) simulation engine named Momentum. Momentum is based on the method-of-moments (MoM) numerical solution of Maxwell's equations [3]. Unlike some EM simulation software Momentum's solutions are presented in the S parameter format that is familiar to the microwave circuit designer. A dataset is created that can be graphed just like any linear simulation. The Momentum model is created from the circuit layout rather than the schematic. In this section we will create a Momentum model from the layout that was created by the linear schematic. However we could import an arbitrary PCB artwork from any CAD program. Right click on the Layout window to expose the Layout Properties. On the General Tab make sure to specify the correct units (mils) that represent the drawing. Also check the 'show EM Box' check box so that a proper enclosure is modeled for the circuit. The box represents a metal enclosure that will serve as the boundary conditions for the EM simulation. The simulator will identify any box resonances that may occur which could have an adverse effect on the circuit design. The box sides must be lined up perpendicular to the input and output ports. The box size (length and width) can be adjusted by entering the desired dimensions in the Box Width (X) and Box Height (Y) settings as shown in Figure 4-50. The box height is specified in the Layers tab as the air above the metal conductor or 250 mils. On the Layer Tab make sure that the microstrip dielectric material is defined on the Substrate line. Once all of the Layer settings have been specified add the Momentum Analysis to the Workspace as shown in Figure 4-52.



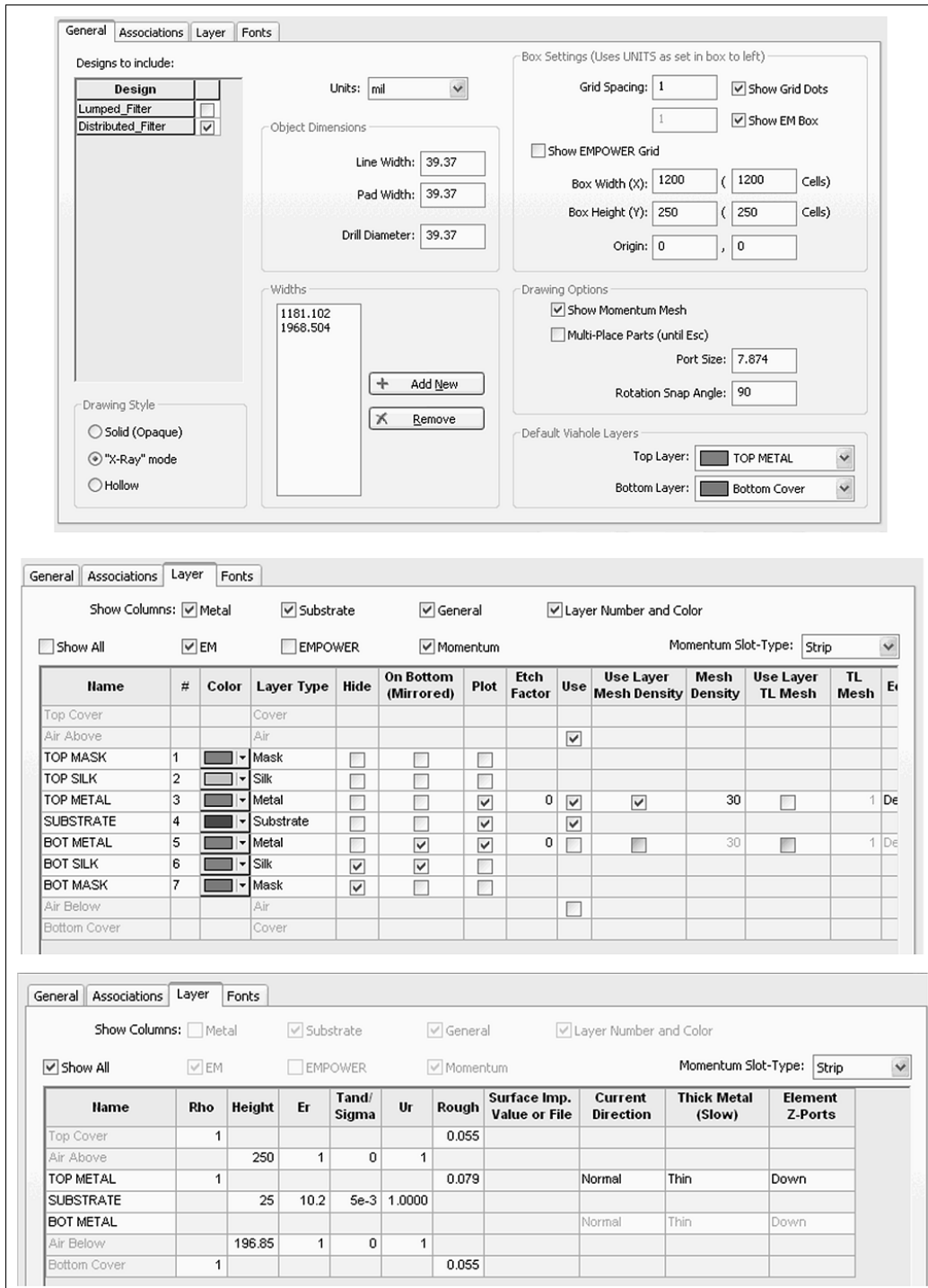


Figure 4-57 General and layer tabs of the layout properties

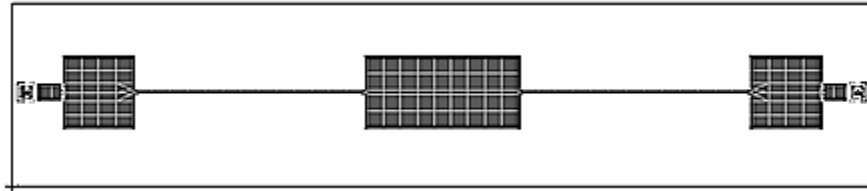


Figure 4-58 Filter layout showing box outline and conductor mesh

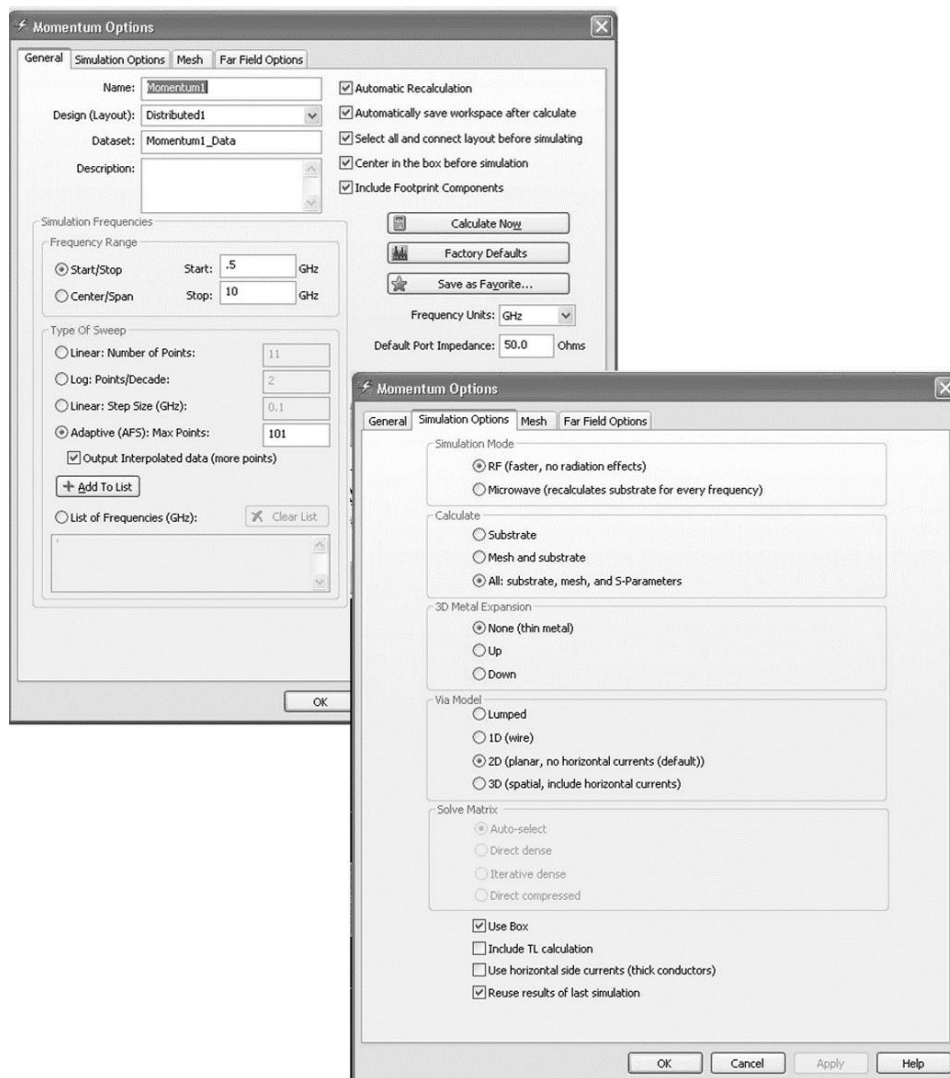
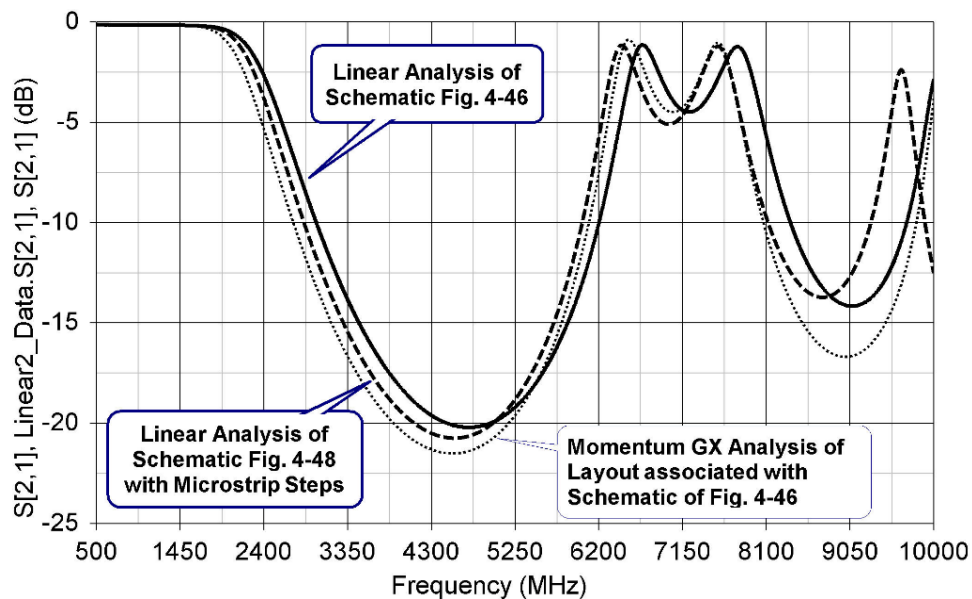


Figure 4-59 Momentum simulation options setup

On the General Tab, set the start and stop frequency for the simulation and select the adaptive sweep type. The adaptive sweep reduces frequency point interpolation error. On the Simulation Options Tab choose the RF simulation mode. The RF simulation mode is a much faster EM simulation and is suitable for lower microwave (RF) frequencies where there is not a significant amount of coupling among transmission lines. The Microwave simulation mode is a full wave EM analysis that includes all coupling radiation within the box. Also check the 'Calculate - All' button so that the metal mesh and the substrate are used in the solution.



**Figure 4-60** Linear simulation and momentum simulation comparison

The comparison between the Linear and Momentum simulations shows that there is some further deviation in the filter rejection as the frequency increases above 2 GHz.

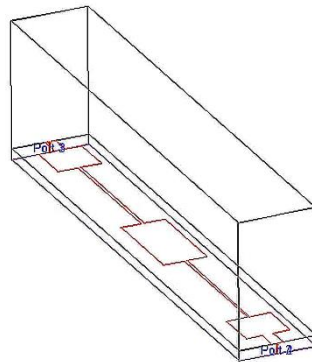


**Figure 4-61** 3D View of filter and prototype filter printed circuit board

#### 4.9.4 Microstrip Edge Coupled Line Filter Design

The edge coupled microstrip line is very popular in the design of bandpass filters. A cascade of half-wave resonators in which quarter wave sections are parallel edge coupled lines, are very useful for realizing narrow band, band pass filters. This type of filter can typically achieve  $\leq 15\%$  fractional bandwidths <sup>[4]</sup>.

**Example 4.9-2:** Design a band pass filter at 10.5 GHz. The filter is designed on RO3010 substrate ( $\epsilon_r = 10.2$ ) with a dielectric thickness of 0.025 inches. The filter should have a pass band of 9.98 – 11.03 GHz. As a design goal the filter should achieve at least 20 dB rejection at 9.65 GHz. In other words the filter is required to have  $> 20$  dB rejection at 330 MHz below the lower passband frequency.

**Solution:** The Passive Circuit DesignGuide utility in ADS is used to design the filter network. The procedure for opening and using the Passive Circuit DesignGuide utility is as follows.

1. In the schematic window, choose DesignGuide > Passive Circuit > Passive Control Window.
2. From Passive Circuit DesignGuide toolbar, choose View > Component Pallet > Microstrip.
3. From Passive Circuit DG – Microstrip pull-down list, choose Filter-Bandpass
4. From Filter-Bandpass pull-down list, choose Chebyshev

5. Set the filter parameters and vary the order until the desired filter rejection is achieved.

The Passive Circuit DesignGuide program shows that a 6<sup>th</sup> order filter should meet the rejection specifications. The synthesized filter schematic and response are shown in Figures 4-61 and 4-62.

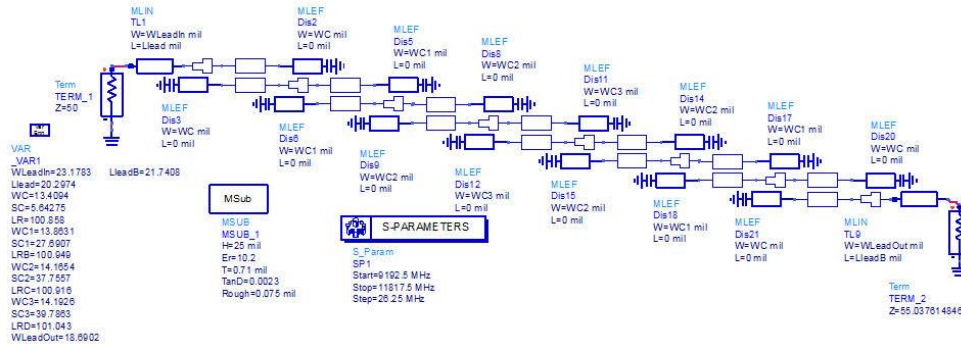


Figure 4-61 Parallel line edge coupled microstrip bandpass filter schematic

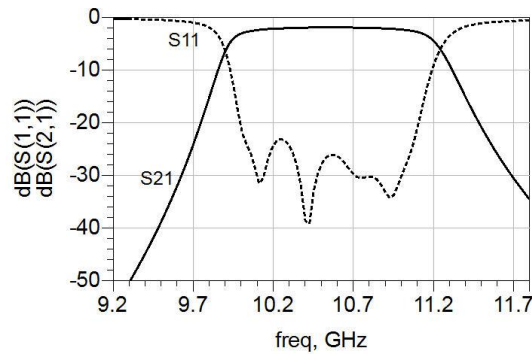


Figure 4-62 Band pass filter response

#### 4.9.5 Electromagnetic Analysis of the Edge Coupled Filter

The designer must be cautious when using Linear Analysis techniques to design circuits with multiple edge coupled microstrip lines. We know that there is a large percentage of the parallel line coupling that occurs in the free space above the microstrip substrate and the conductors. This can lead to considerable error when relying on the linear simulation results. The coupled line models used by the

linear simulator are based on closed form expressions derived from coupling measurements on parallel lines with loosely defined boundary conditions.

**Example 4.9-3:** Use the microwave mode in the Momentum software to simulate the edge coupled filter.

**Solution:** Using the circuit model created in the last section examine the layout of the filter. On the Layout-Properties window, make sure that the “Show EM Box” is selected. Then adjust the size of the box to fit the filter. Set the filter box width (Y) to 400 mils and the box height (X dimension) to 760 mils. The EM box will show up as a red rectangle on the layout window. Next edit the Layer tab. Check the “Show All” box. Scroll across to make sure that the substrate thickness, dielectric constant, and loss tangent parameters are correct. Check “Use” boxes as appropriate. Set the initial box height (Z dimension) at 300 mils.

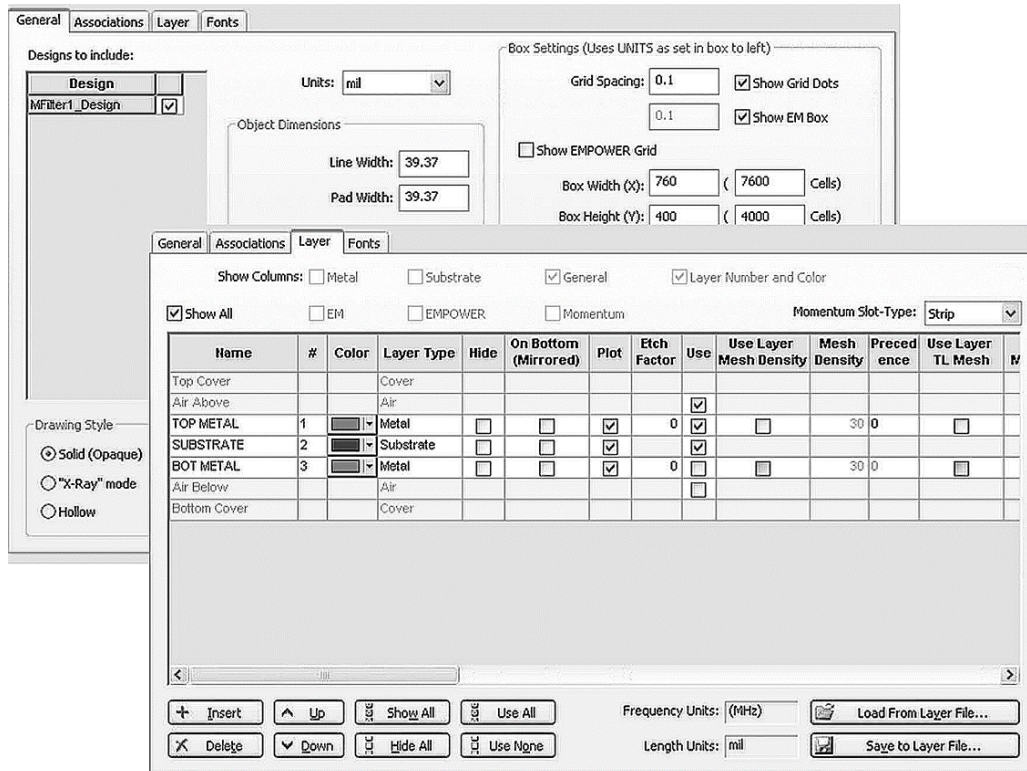


**Figure 4-63** Layer setup for momentum analysis of edge coupled filter

Add a Momentum GX Analysis to the workspace and set the parameters as shown in Figure 4-64. Set the analysis frequency range of 9 to 12 GHz with an Adaptive sweep type. On the Simulation Options tab, make sure that the “use box” check box has been selected. This forces a 3D mesh of the entire filter and box. This time we must select the microwave simulation mode so that the box radiation effects are properly modeled.

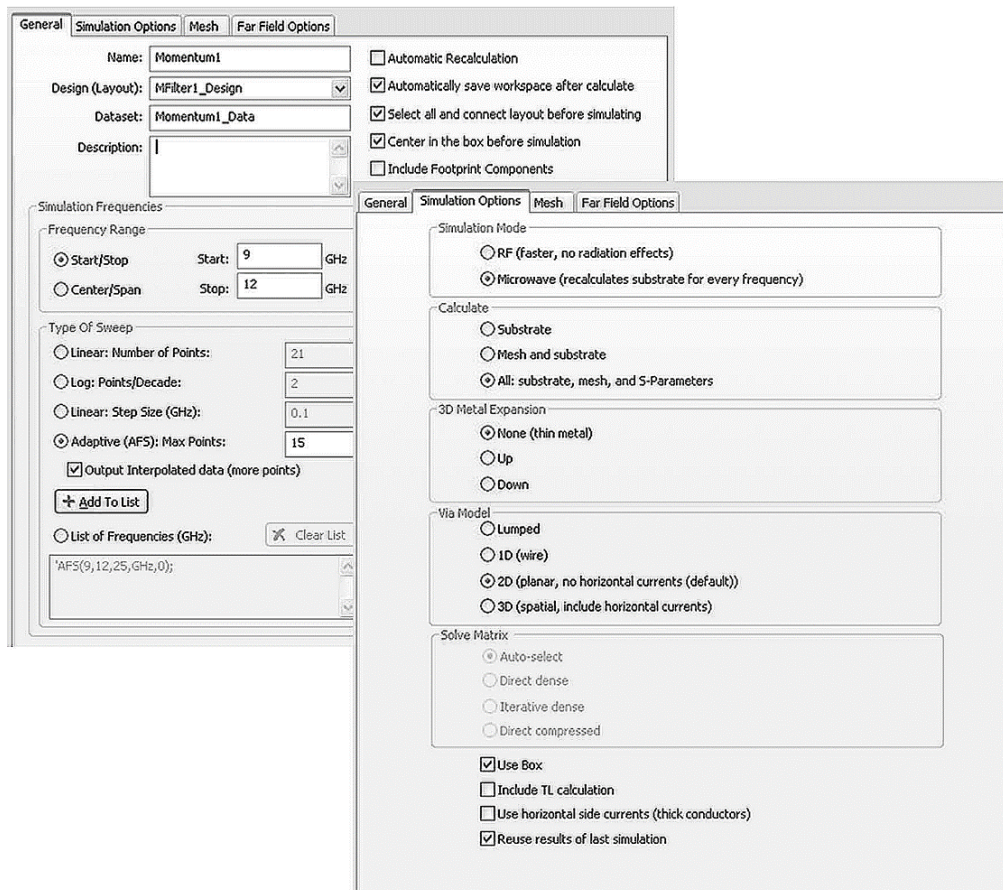


**Figure 4-64** Momentum GX general setup

Perform a Momentum simulation on the filter and observe the response. The edge-coupled filter is particularly sensitive to the sidewalls providing the proper boundary conditions for the coupled energy between the parallel-coupled lines. Begin the tuning process by first reducing the box height to 250 mils. Keep the cover height at 250 mils. A 3D picture of the filter is shown in Figure 4-66 to have a good appreciation of the physical geometry of the filter. Figure 4-65 shows the comparison between the linear model and the Momentum EM model. We see that the actual pass band is shifted up in frequency slightly while the bandwidth

has been reduced. Varying the box dimensions shows that the filter skirts are heavily dependent on the box around the filter.

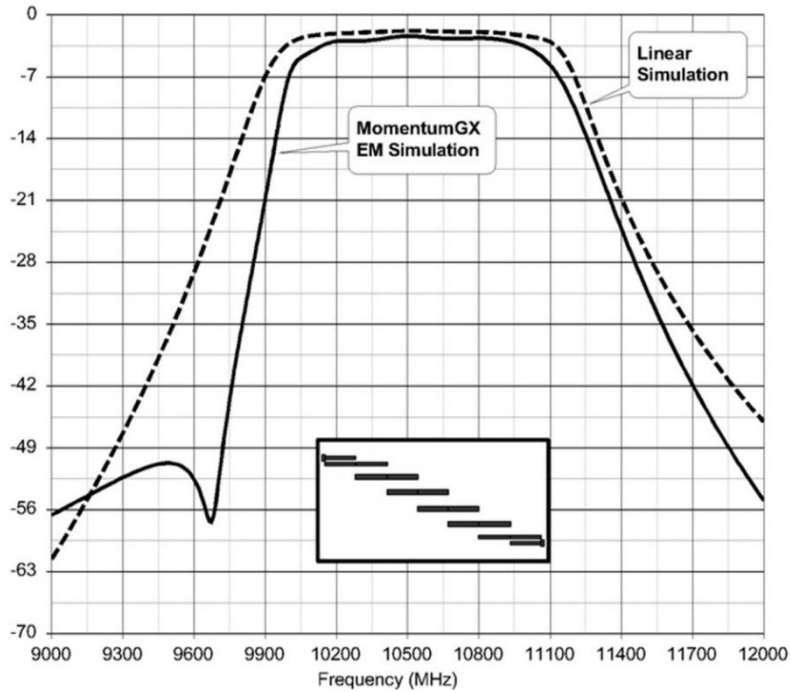


**Figure 4-65** Comparison between the linear and the Momentum EM model

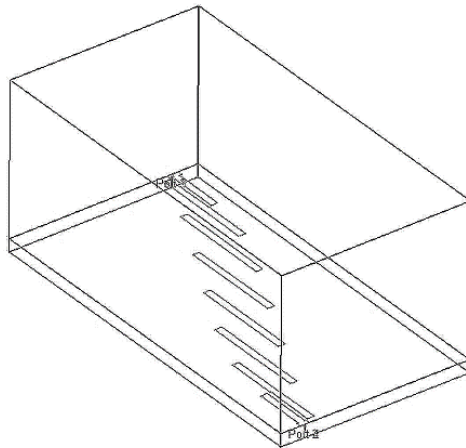


**Figure 4-66** 3D View of the edge coupled filter showing layer stack



## **References and Further Readings**

- [1] *Handbook of Filter Synthesis*, Anatol I. Zverev, Wiley 1967
- [2] *RF Circuit Design*, Second Edition, Christopher Bowick, Elsevier 2008
- [3] Keysight Technologies, Manuals for Advanced Design System, *ADS 2015.07 Documentation Set*, EEsof EDA Division, Santa Rosa, California  
[www.keysight.com](http://www.keysight.com)
- [4] *Foundations for Microstrip Circuit Design*, T.C. Edwards, John Wiley & Sons, New York, 1981
- [5] *Q Factor*, Darko Kajfez, Vector Fields, Oxford Mississippi, 1994
- [6] David M. Pozar, *Microwave Engineering*, Third Edition, John Wiley and Sons, Inc. 2005
- [7] *Q Factor Measurement with Network Analyzer*, Darko Kajfez and Eugene Hwan, IEEE Transactions on Microwave Theory and Techniques, Vol. MTT-32, No. 7, July 1984.
- [8] *High Frequency Techniques*, Joseph F. White, John Wiley & Sons, Inc., 2005
- [9] *Soft Substrates Conquer Hard Designs*, James D. Woermbke, Microwaves, January 1982.
- [10] *Principles of Microstrip Design*, Alam Tam, RF Design, June 1988.
- [11] Ali A. Behagi and Stephen D. Turner, *Microwave and RF Engineering, A Simulation Approach with Keysight Genesys Software*, BT Microwave LLC, State College, PA , March 2015

## **Problems**

- 4-1. Consider the one port resonator that is represented as a series RLC circuit as shown. Analyze the circuit, with  $R = 5 \Omega$ ,  $L = 5 \text{ nH}$ , and  $C = 5 \text{ pF}$ . Plot the magnitude of the resonator input impedance and measure the resonance frequency.
- 4-2. Consider the one port resonator that is represented as a parallel RLC circuit as shown. Analyze the circuit, with  $R = 500 \Omega$ ,  $L = 50 \text{ nH}$ , and  $C = 50 \text{ pF}$ . Plot the magnitude of the resonator input impedance and measure the resonance frequency.
- 4-3. Design a Butterworth lowpass filter having a passband of 2 GHz with an attenuation 20 dB at 4 GHz. Plot the insertion loss versus frequency from 0 to 5 GHz. The system impedance is  $50 \Omega$ .
- 4-4. Design a 5<sup>th</sup> order Chebyshev highpass filter having 0.2 dB equal ripples in the passband and cutoff frequency of 2 GHz. The system impedance is  $75 \Omega$ . Plot the insertion loss versus frequency from 0 to 5 GHz.
- 4-5. In a full duplex communication link, the uplink signal is around 200 MHz while the downlink is at 500 MHz. A 25 Watt power amplifier is used on the uplink with 20 dB gain.
- (a) Design a low pass filter on the uplink to pass the 200 MHz uplink signal while rejecting any noise power in the 500 MHz band. Design the passband cutoff frequency is at 220 MHz, therefore, the filter should have a Chebyshev Response with 0.1 dB pass band ripple. The reject requirement is at least -40 dB rejections at 500 MHz.
- (b) Design a High Pass Filter that passes frequencies in the 480 MHz to 520 MHz range. The High Pass Filter specifications are: The passband cutoff frequency is 480 MHz, therefore, the filter should have a Chebyshev response with 0.1 dB pass band ripple. The reject requirement is at least -60 dB losses at 190 MHz.

- 4-6. Design a  $75 \Omega$  transmission line of sufficient length to act as a 10 nH inductor. Calculate the microstrip line width on the Rogers 0.025 inch RO3010 material.
- 4-7. Using the microwave filter synthesis tool, design a stepped impedance low pass filter on RO3003 material that is 0.010 inches thick. Use a Chebyshev response with a 0.01dB ripple and a cutoff frequency of 4 GHz. Determine the worst case in band return loss and the rejection at 6 GHz.
- 4-8. For the filter design of Problem 4-7 create an EM simulation using Momentum. Compare the EM simulation to a linear simulation. Comment on the rejection comparison at 6 GHz.
- 4-9. For the filter design of Problem 4-7 determine the frequencies at which reentrant modes exist up through 20 GHz.
- 4-10. Design a half wave microstrip resonator at 10 GHz using RO3003 substrate that is 0.020 thick. Initially design the resonator with a 50  $\Omega$  line impedance. Select a coupling capacitor to critically couple the resonator to the 50  $\Omega$  source. Then determine the resonator line impedance that results in the highest unloaded  $Q_0$ .
- 4-11. Use the microwave filter synthesis tool to design a parallel edge coupled filter on RO3003 substrate that is 0.010 thick. Use a Chebyshev characteristic with 0.10 dB ripple. Design the passband to cover 10.7 GHz to 12.2 GHz. Determine the filter order required to achieve 30 dB rejection at 9 GHz.
- 4-12. For the filter design of Problem 4-10, create an EM simulation using Momentum. Compare the linear and EM simulations. Determine the minimum box width (EM Box height, Y) that creates a box resonance frequency. What is the frequency of the box resonance?

## About the Author

**Ali A. Behagi** received the Ph.D. degree in electrical engineering from the University of Southern California and the MS degree in electrical engineering from the University of Michigan. He has several years of industrial experience with Hughes Aircraft and Beckman Instruments. Dr. Behagi joined Penn State University as an associate professor of electrical engineering in 1986. He has devoted over 20 years to teaching RF and microwave engineering courses and directing university research projects. While at Penn State he received a National Science Foundation equipment grant to establish the RF and microwave engineering lab. He also received the RF and microwave engineering software grant, from Hewlett Packard, to use the software in classroom teaching and laboratory experiments. After retirement from Penn State he has been active as an educational consultant. Dr. Behagi is a Keysight Certified Expert, a senior member of the Institute of Electrical and Electronics Engineers (IEEE), and the Microwave Theory and Techniques Society.